

Supplementary Information

Self-Assembling PEGylated Mannolipids for Liposomal Drug Encapsulation of Natural Products

Self-Assembling PEGylated Mannolipids for Liposomal Drug Encapsulation of Natural Products

Leila Mousavifar,^{a,†} Mukul R. Gupta,^{a,†} Madleen Rivat,^a Aly El Riz,^a Abdelkrim Azzouz,^a Jordan D. Lewicky,^b Alexandrine L. Martel,^b Hoang-Thanh Le,^{b,c,d} René Roy^{a,*}

^a *Glycosciences and Nanomaterial Laboratory, Université du Québec à Montréal, P.O. Box 8888, Succ. Centre-Ville, Montréal, Québec, Canada, H3C 3P8*

^b *Health Sciences North Research Institute, 56 Walford Road, Sudbury, ON, Canada, P3E 2H2*

^c *Medicinal Sciences Division, NOSM University, 935 Ramsey Lake Road, Sudbury, ON P3E 2C6, Canada.*

^d *School of Natural Sciences, Laurentian University, 935 Ramsey Lake Road, Sudbury, ON P3E 2C6, Canada.*

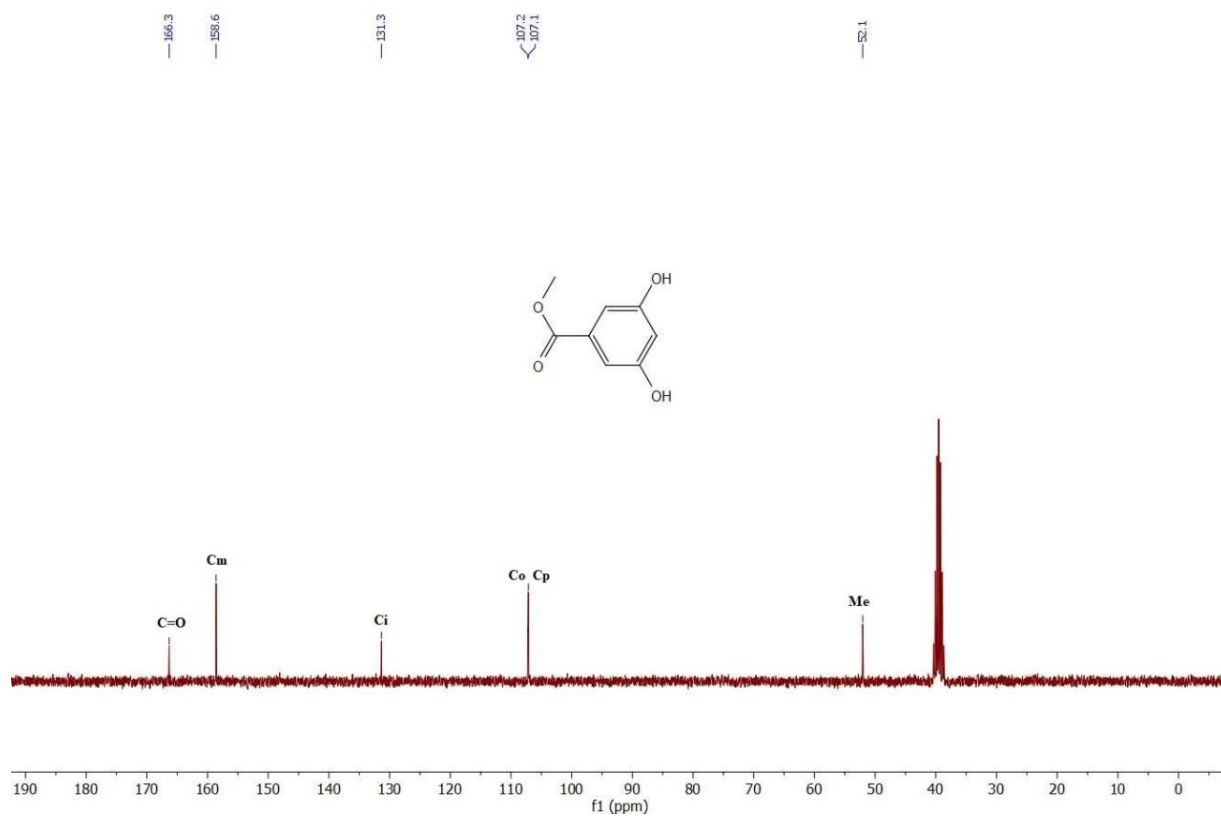
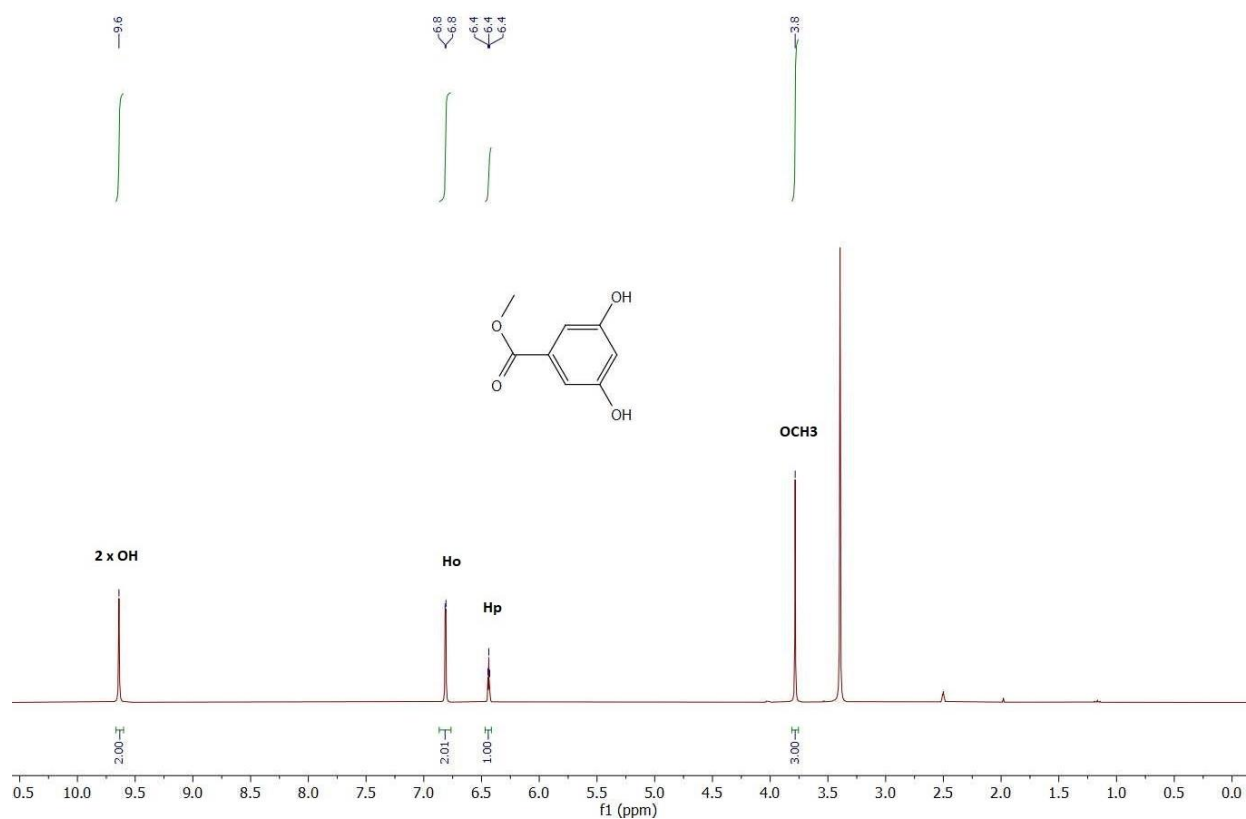
[†] These authors contributed equally.

TABLE OF CONTENTS

NMR Spectra of synthesized compounds:.....2-17

Critical Micelle Concentration (CMC):.....18-20

NMR Spectra of synthesized compounds:



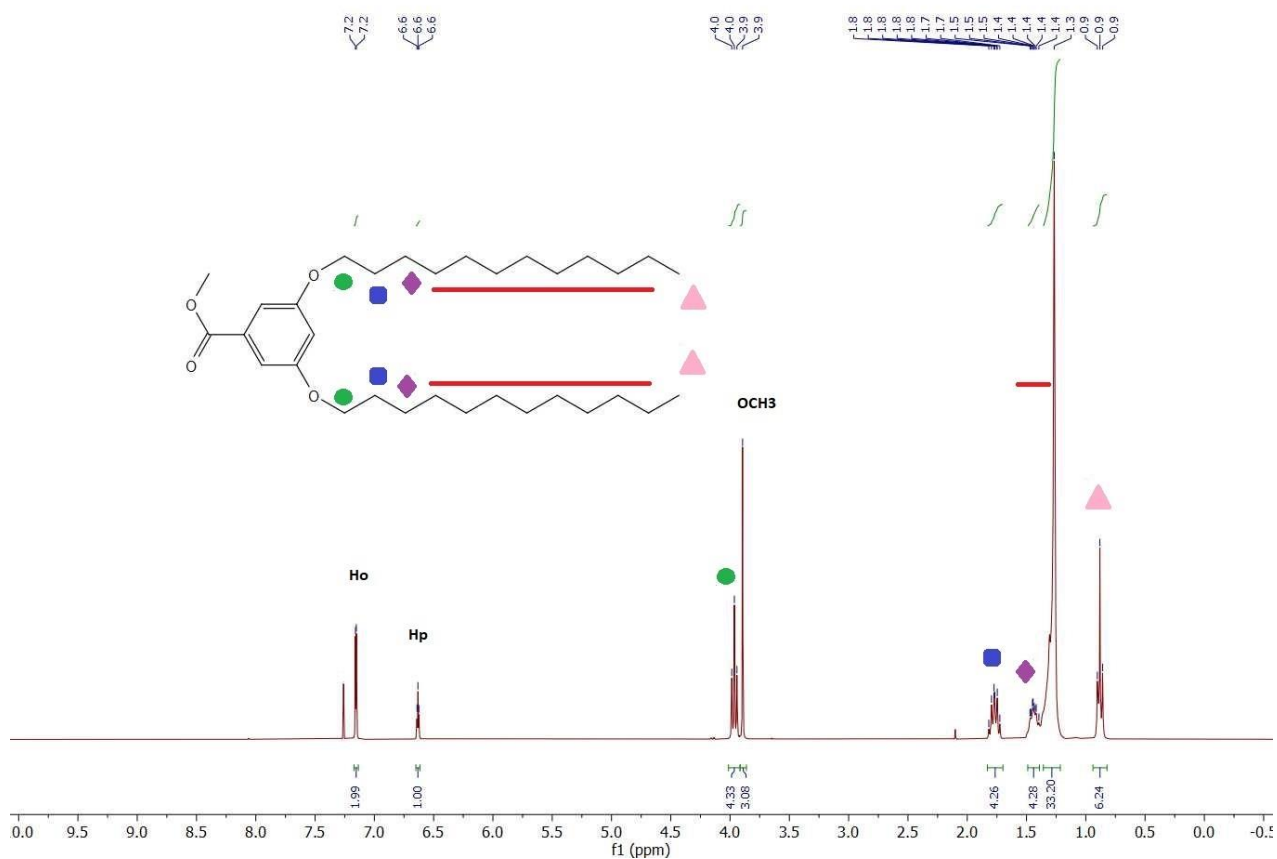


Figure 3. ¹H NMR (300 MHz, CDCl₃) of compound 3

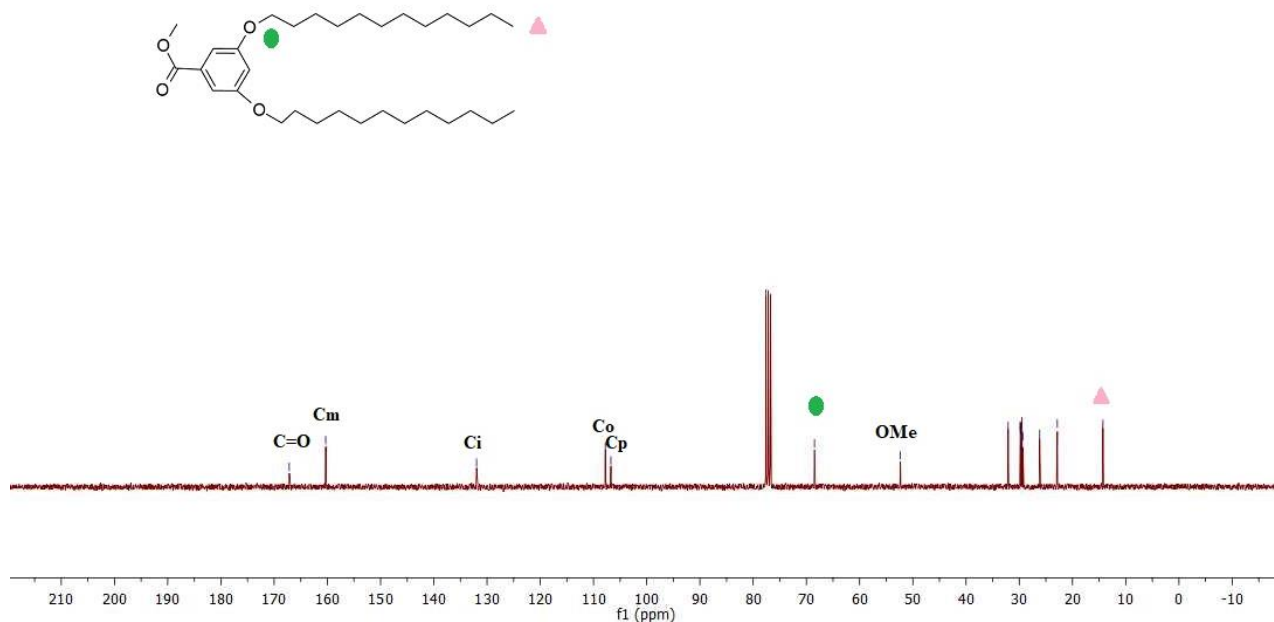


Figure 4. ¹³C-NMR (75 MHz, DMSO-d₆) of compound 3

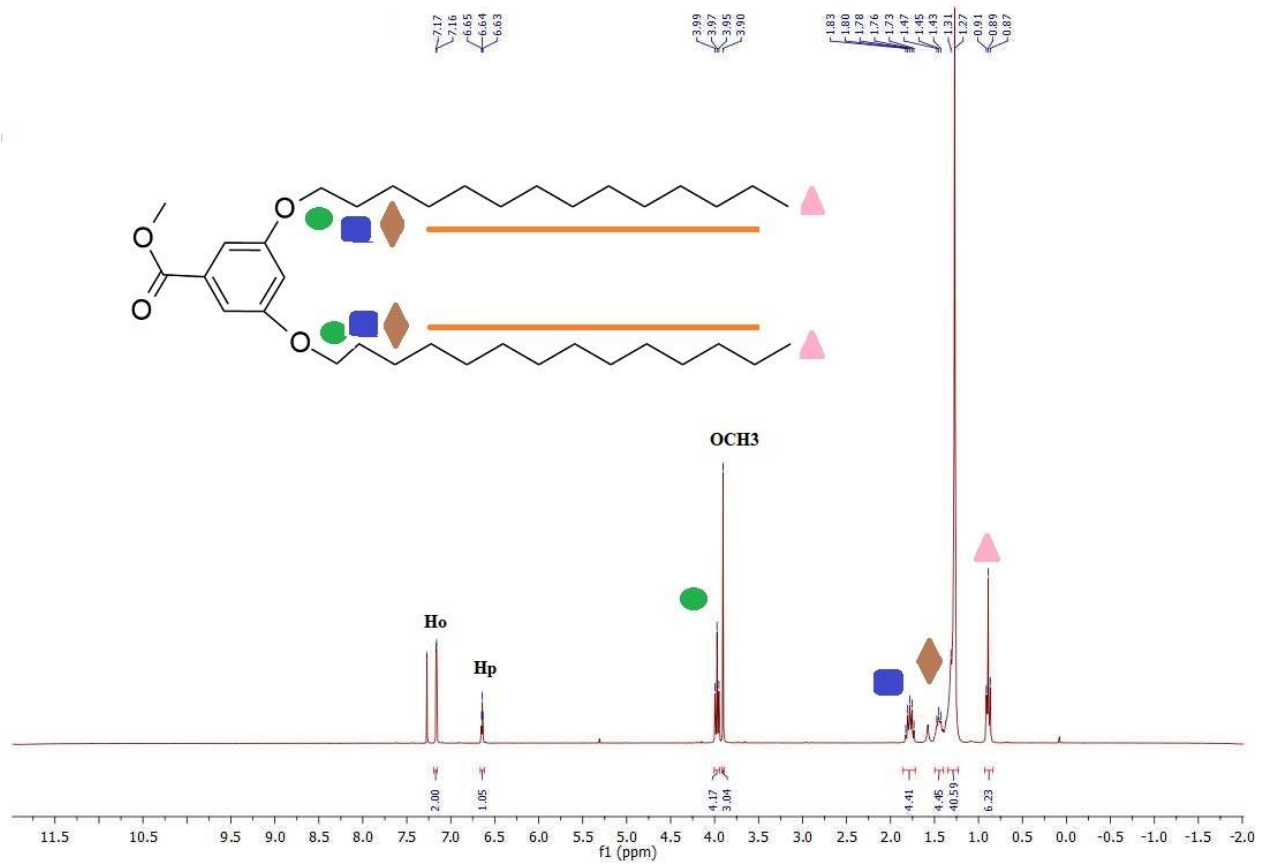


Figure 5. ^1H NMR (300 MHz, CDCl_3) of compound 4

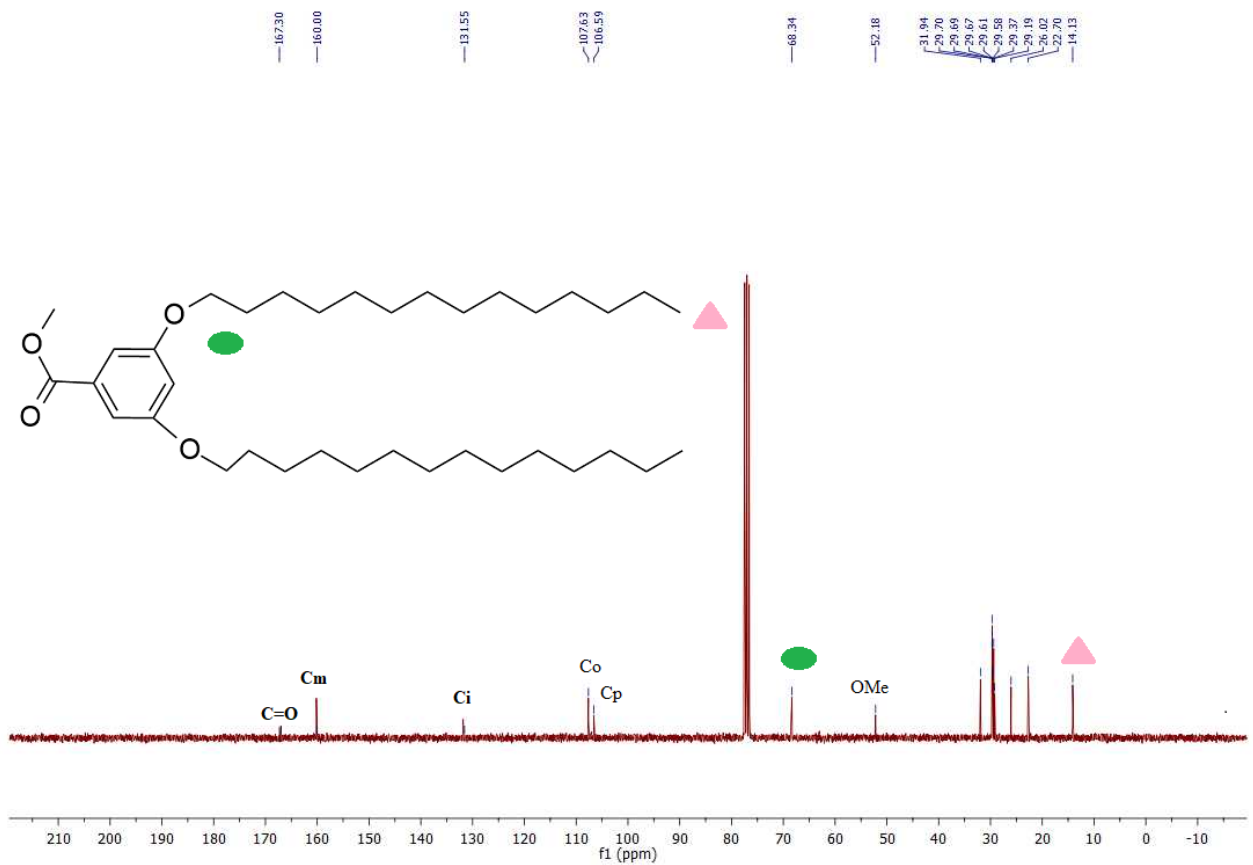
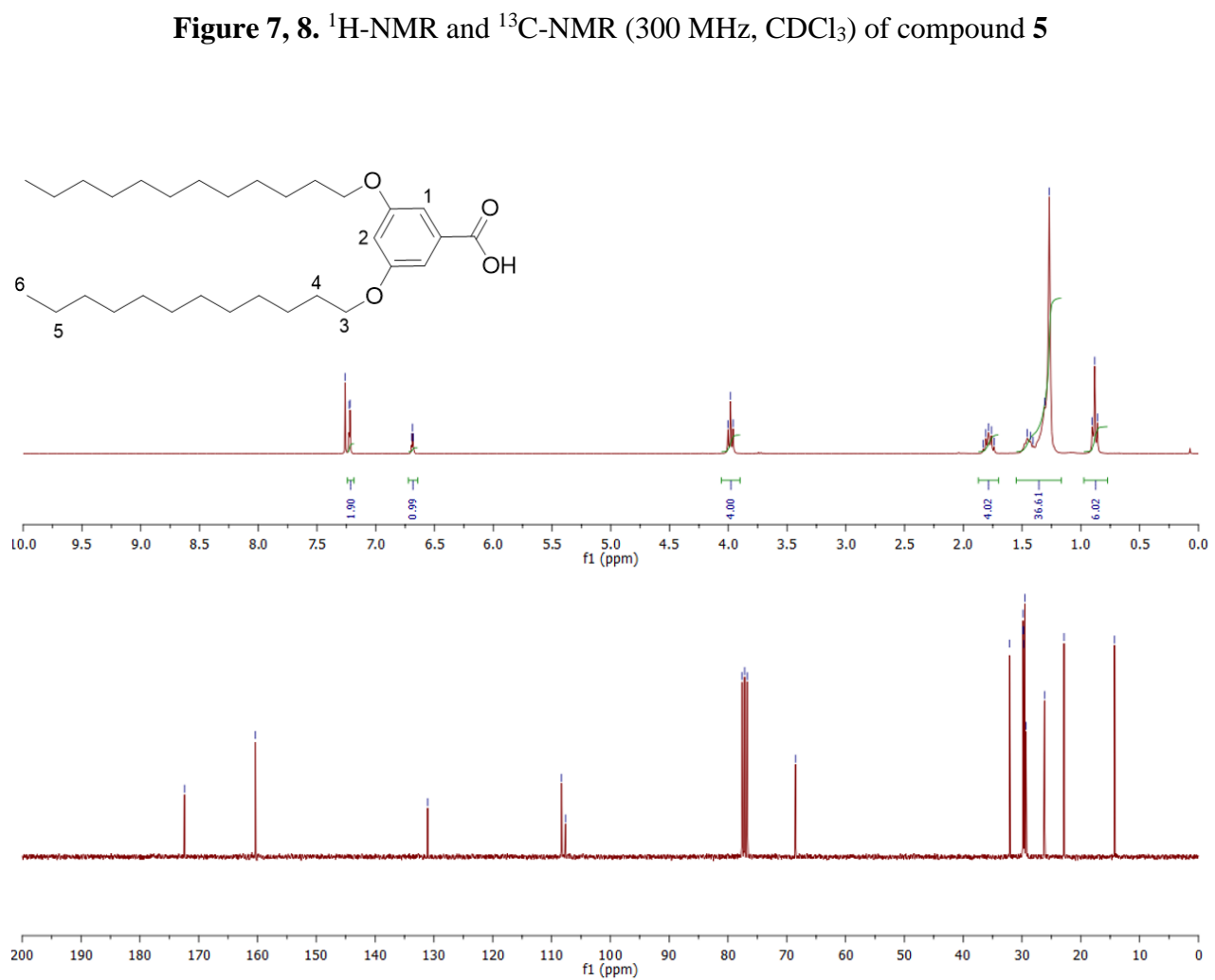
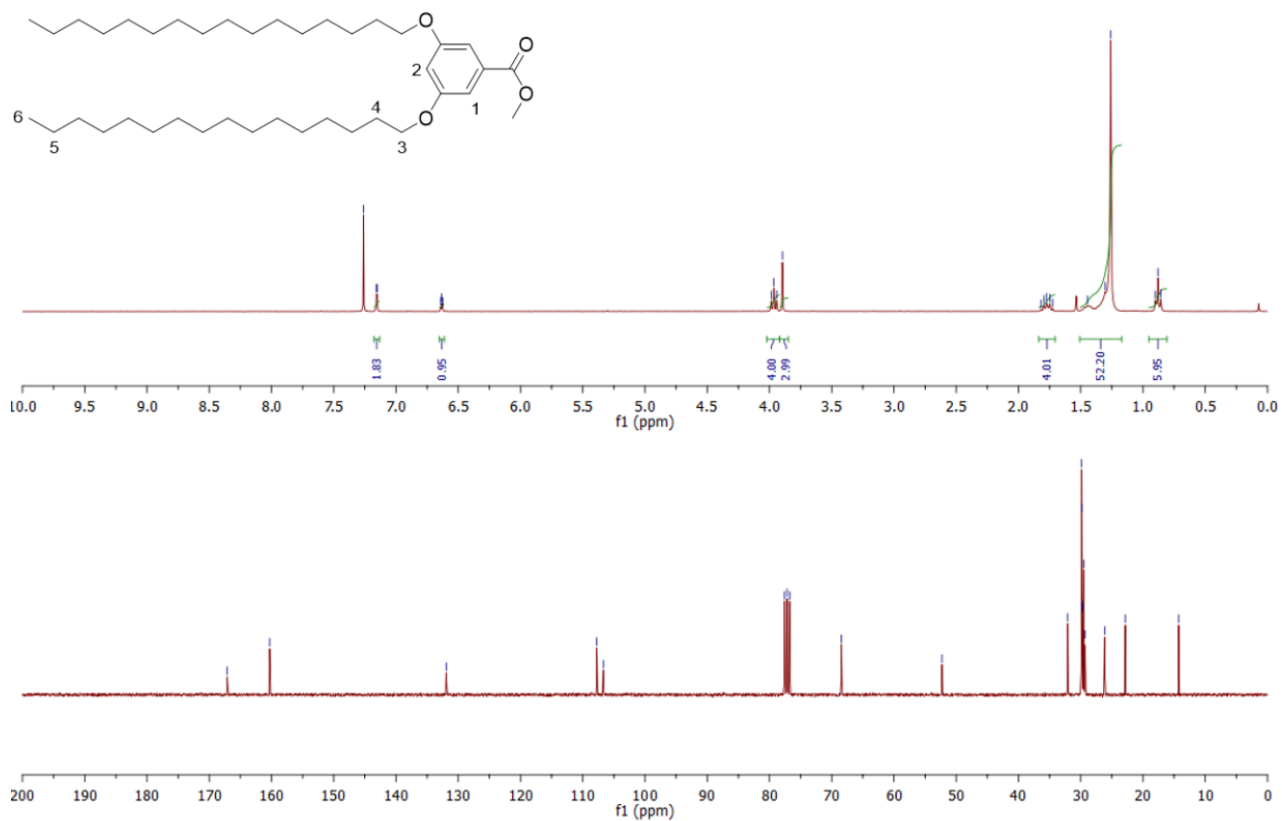
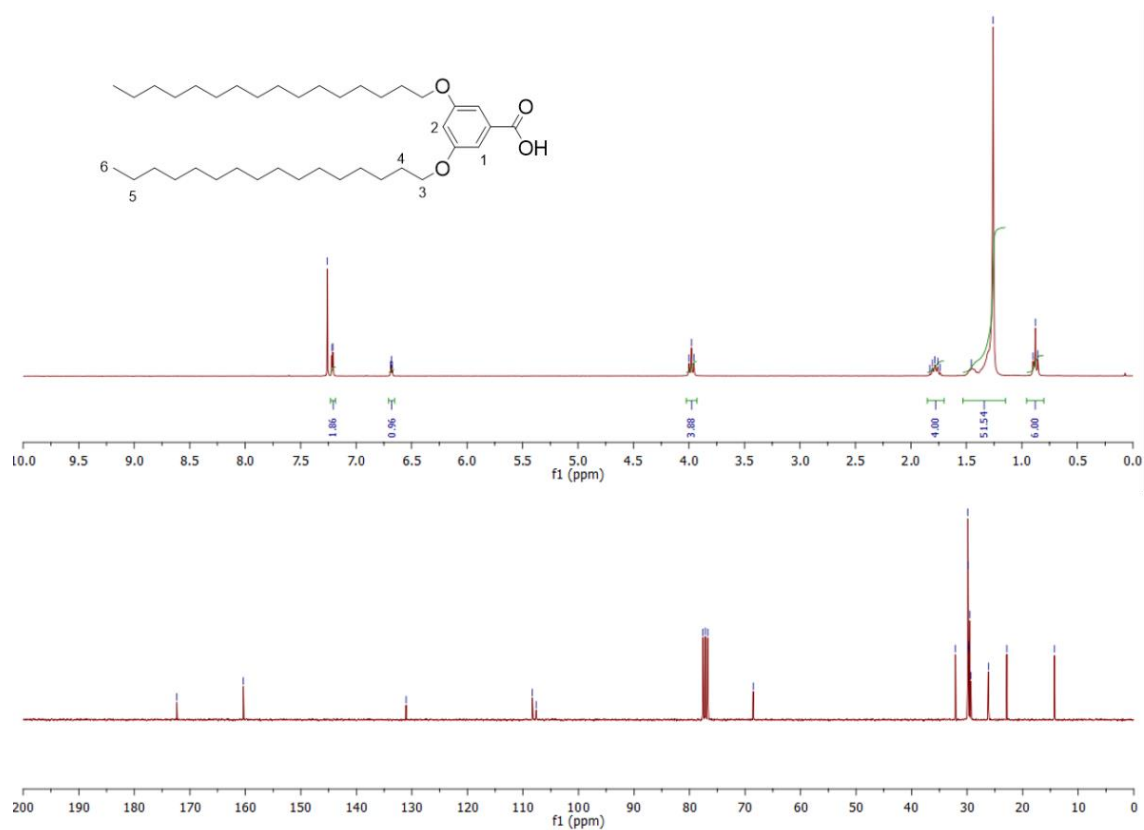
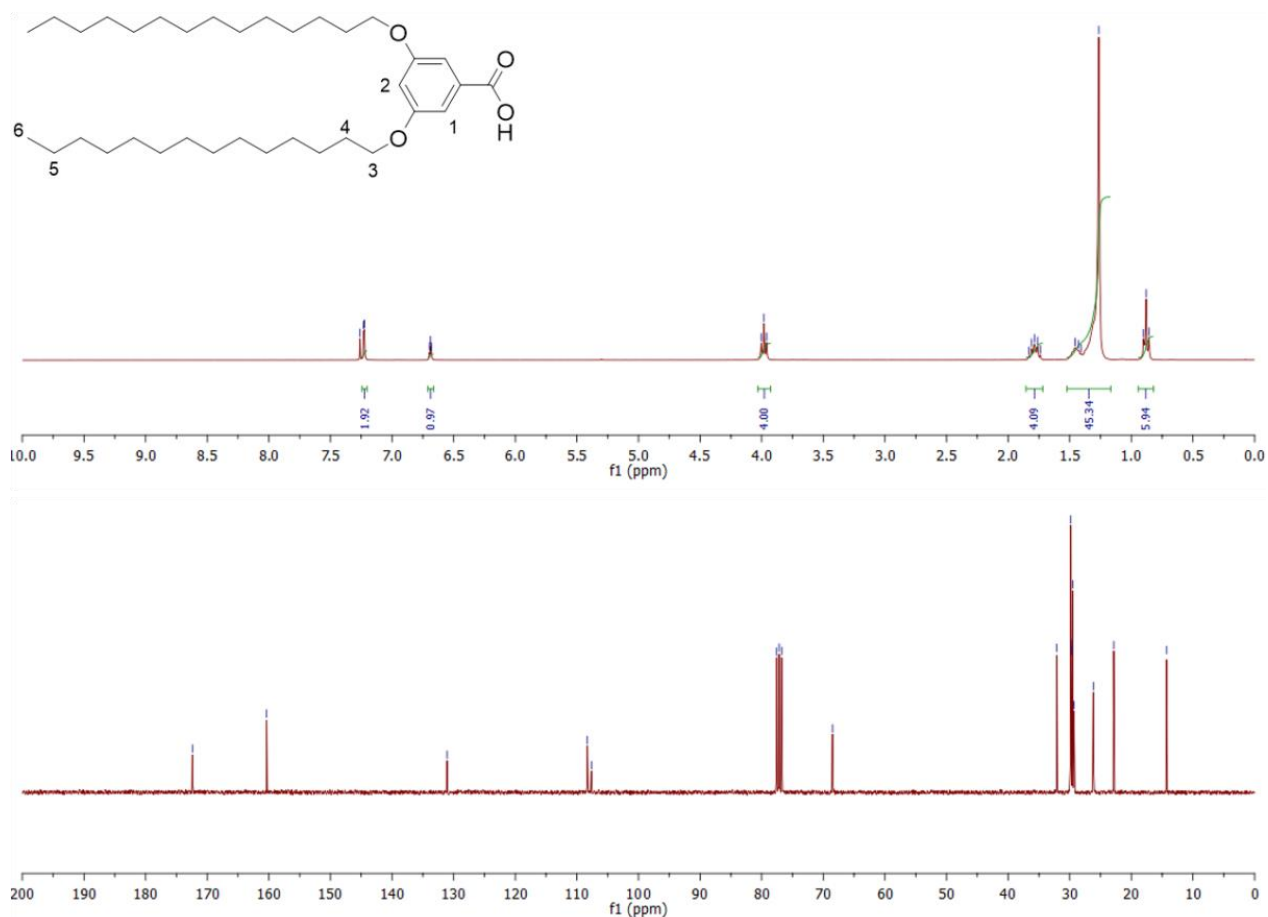


Figure 6. ^{13}C -NMR (300 MHz, CDCl_3) of compound 4





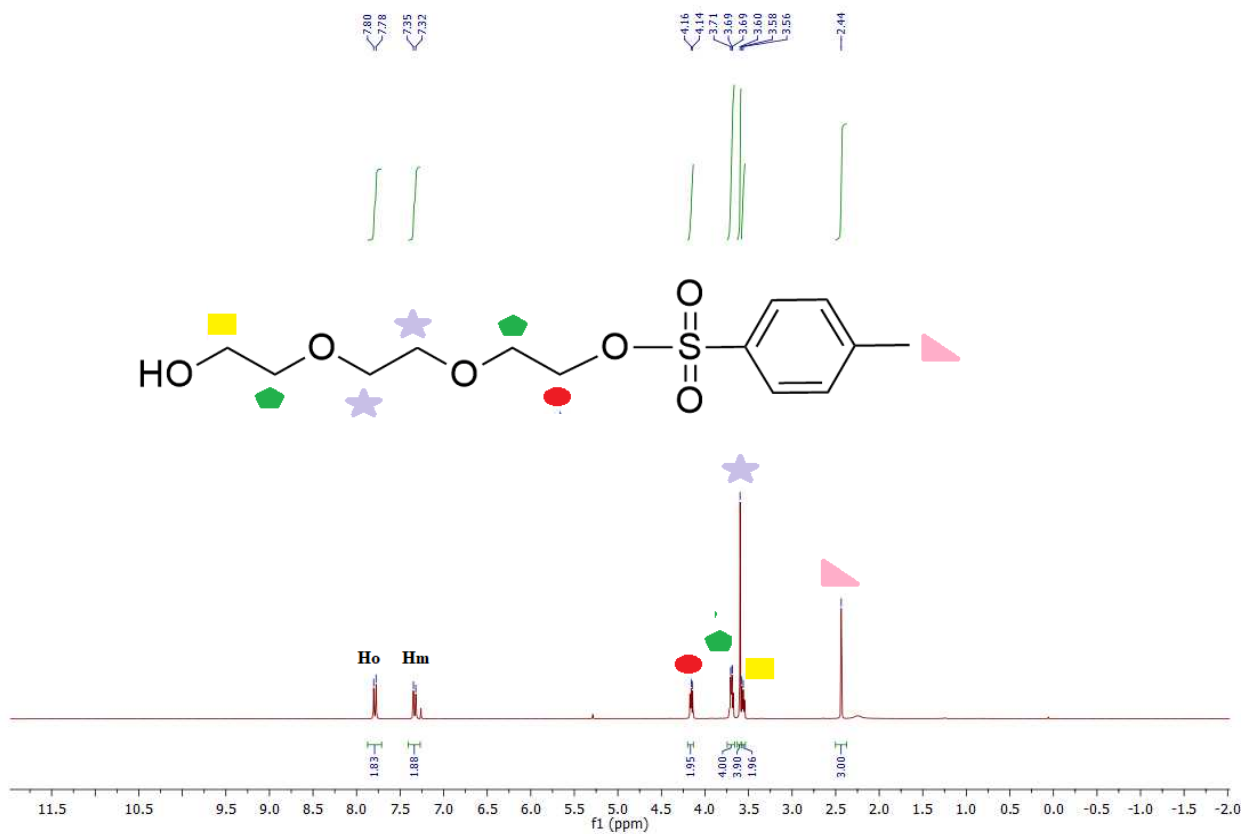


Figure 15. $^1\text{H-NMR}$ (300 MHz, CDCl_3) of compound 10

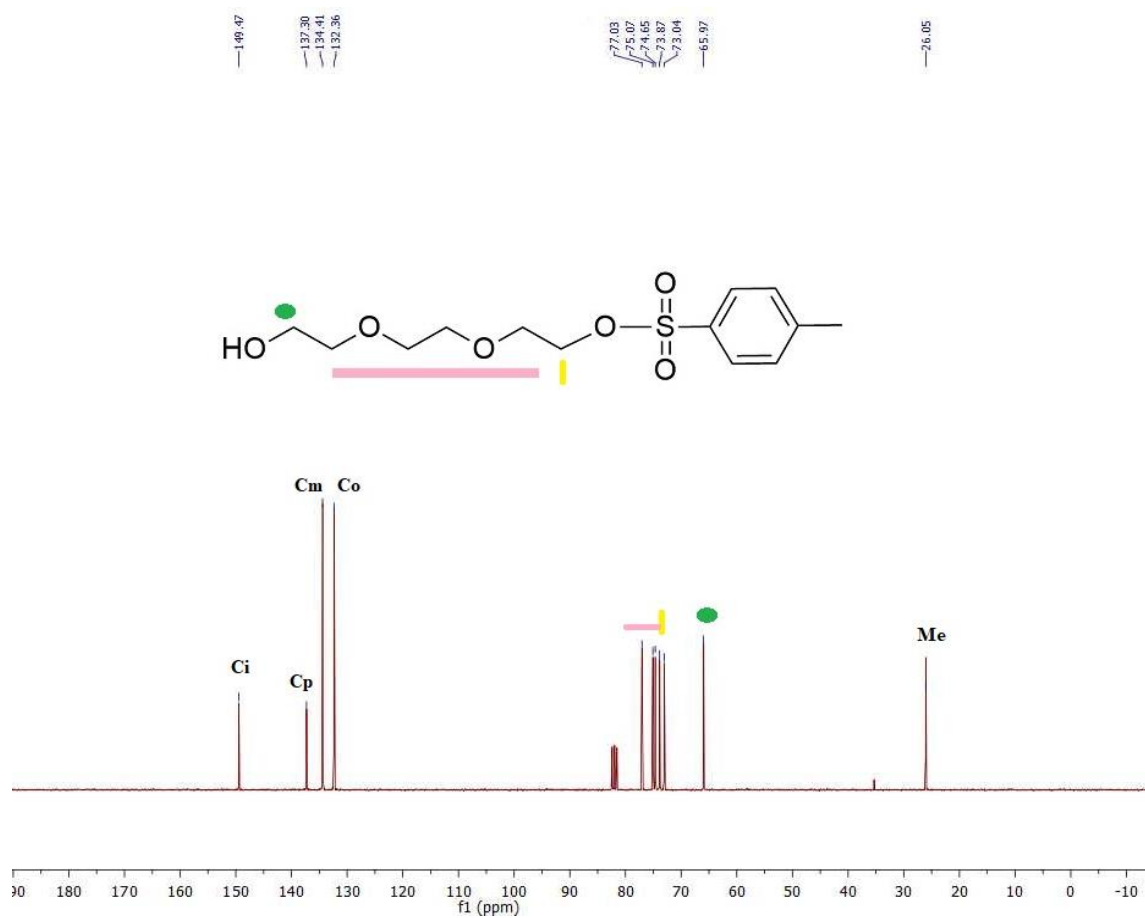


Figure 16. $^{13}\text{C-NMR}$ (300 MHz, CDCl_3) of compound 10

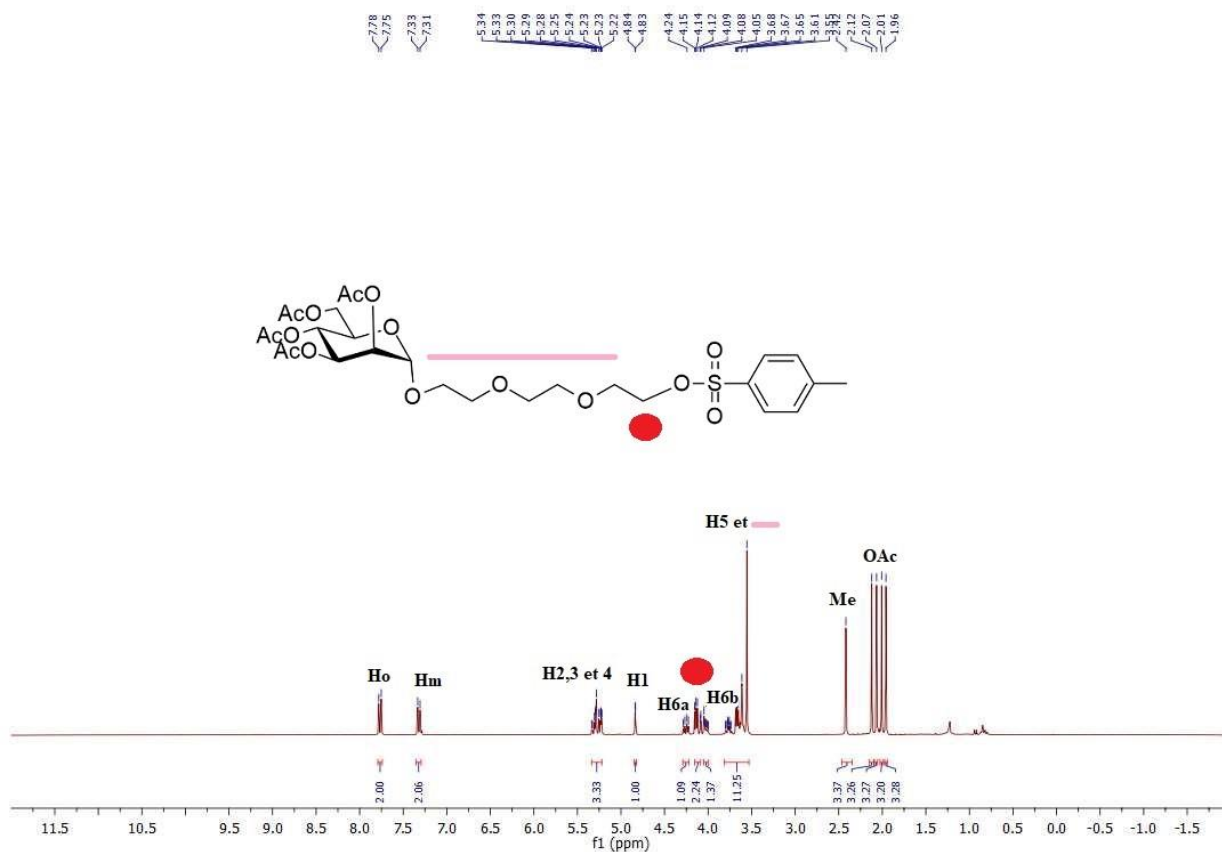


Figure 17. $^1\text{H-NMR}$ (300 MHz, CDCl_3) of compound 12

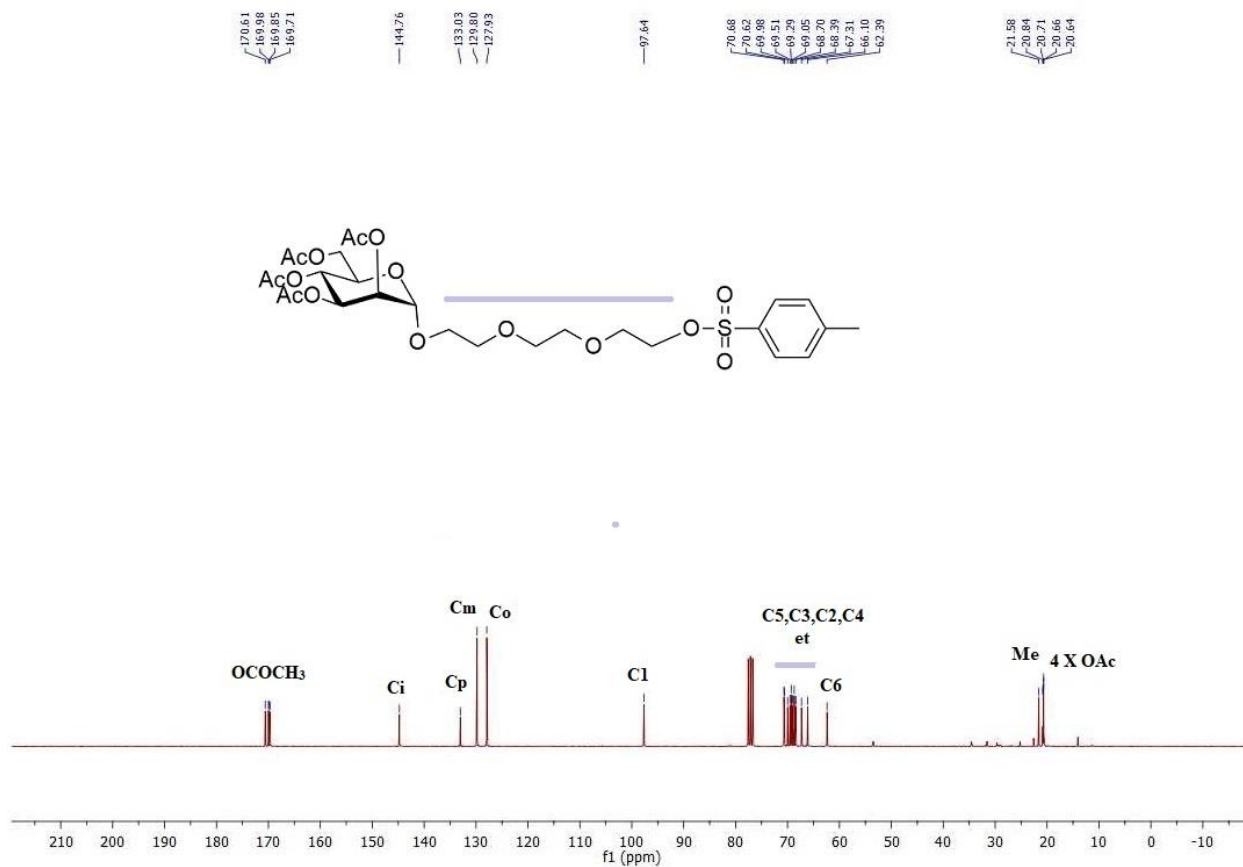


Figure 18. $^{13}\text{C-NMR}$ (300 MHz, CDCl_3) of compound 12

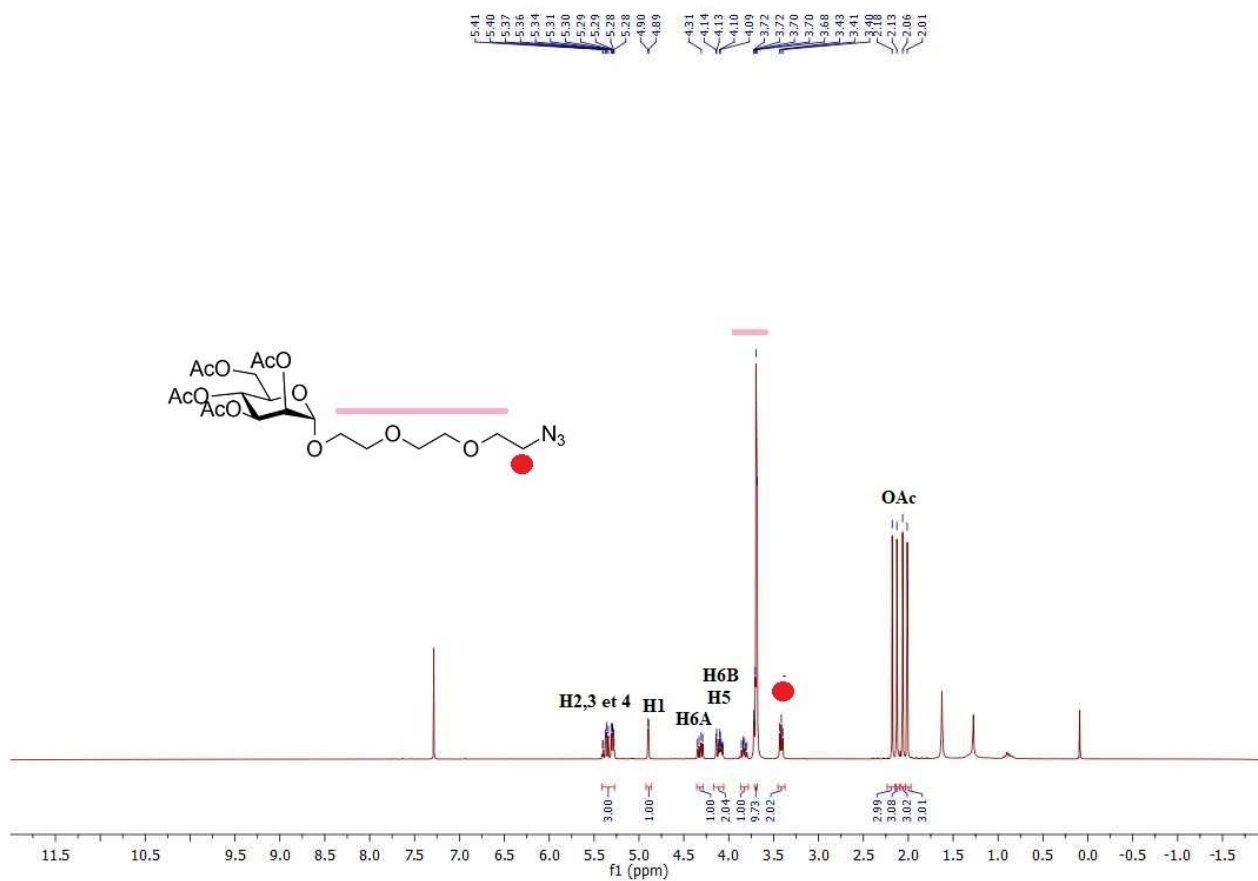


Figure 19. ¹H-NMR (300 MHz, CDCl₃) of compound 13

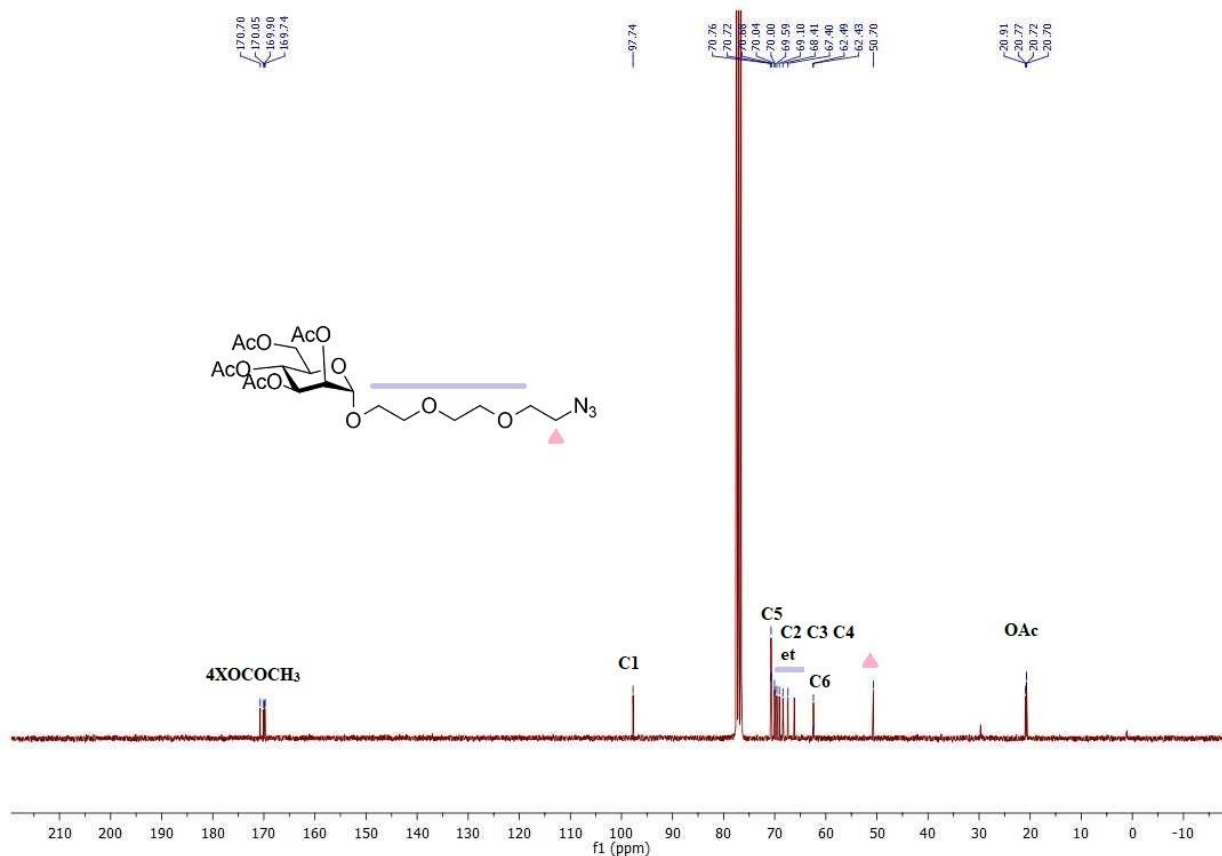


Figure 20. ¹³C-NMR (300 MHz, CDCl₃) of compound 13

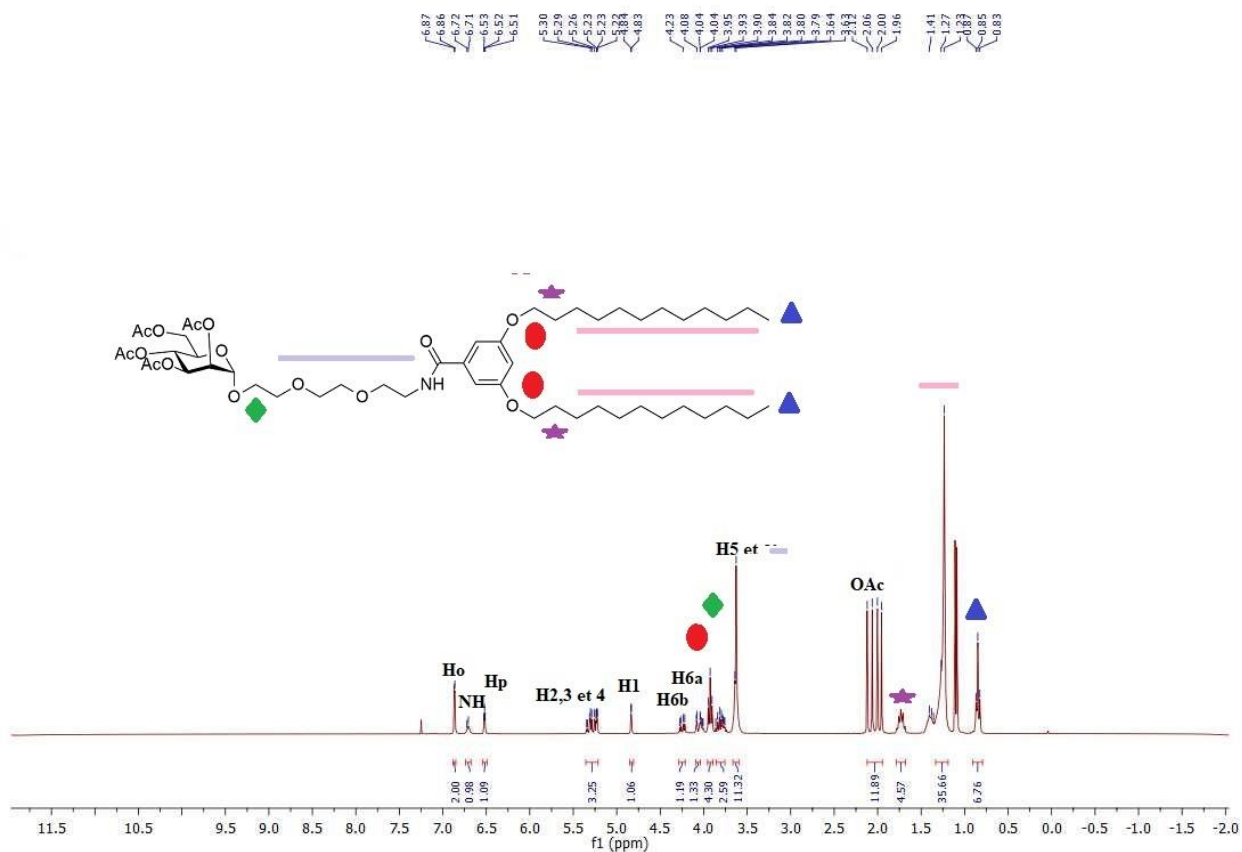


Figure 21. $^1\text{H-NMR}$ (300 MHz, CDCl_3) of compound 14

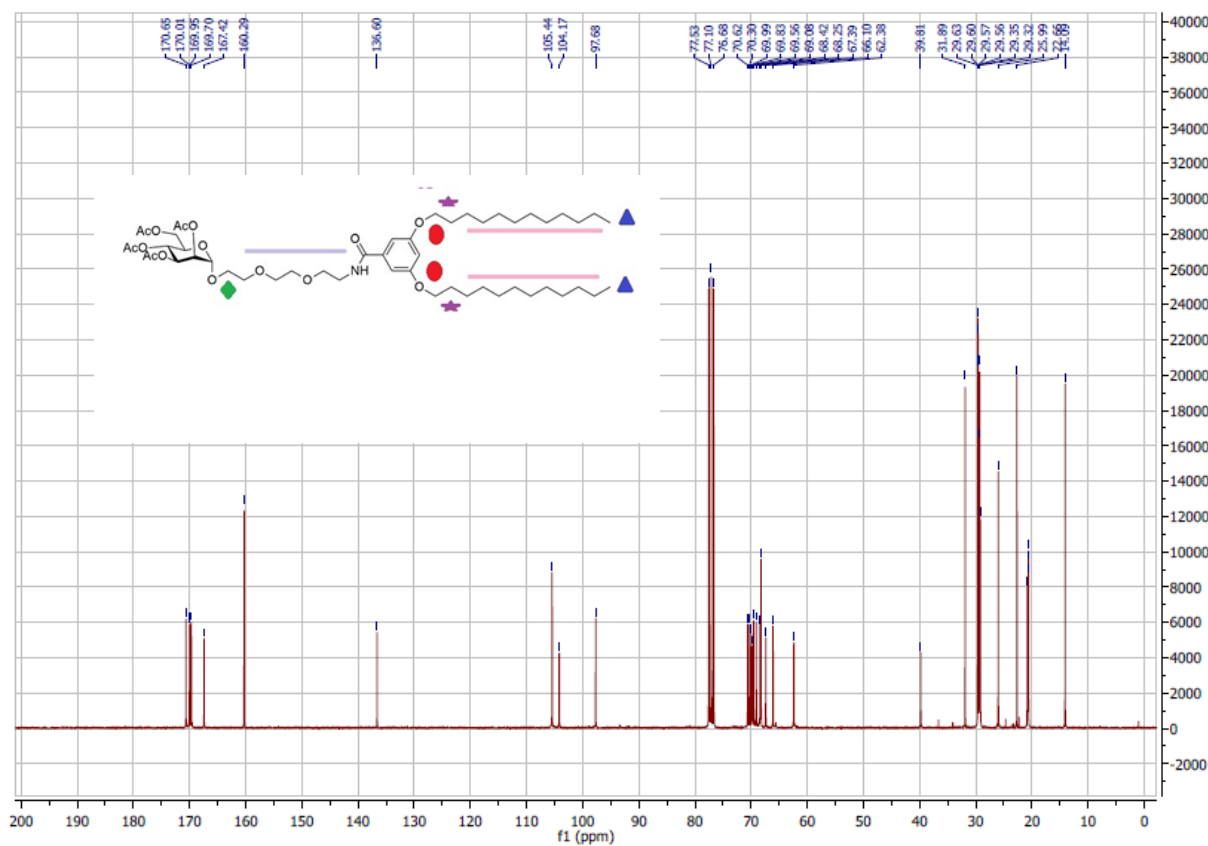


Figure 22. $^{13}\text{C-NMR}$ (75 MHz, CDCl_3) of compound 14

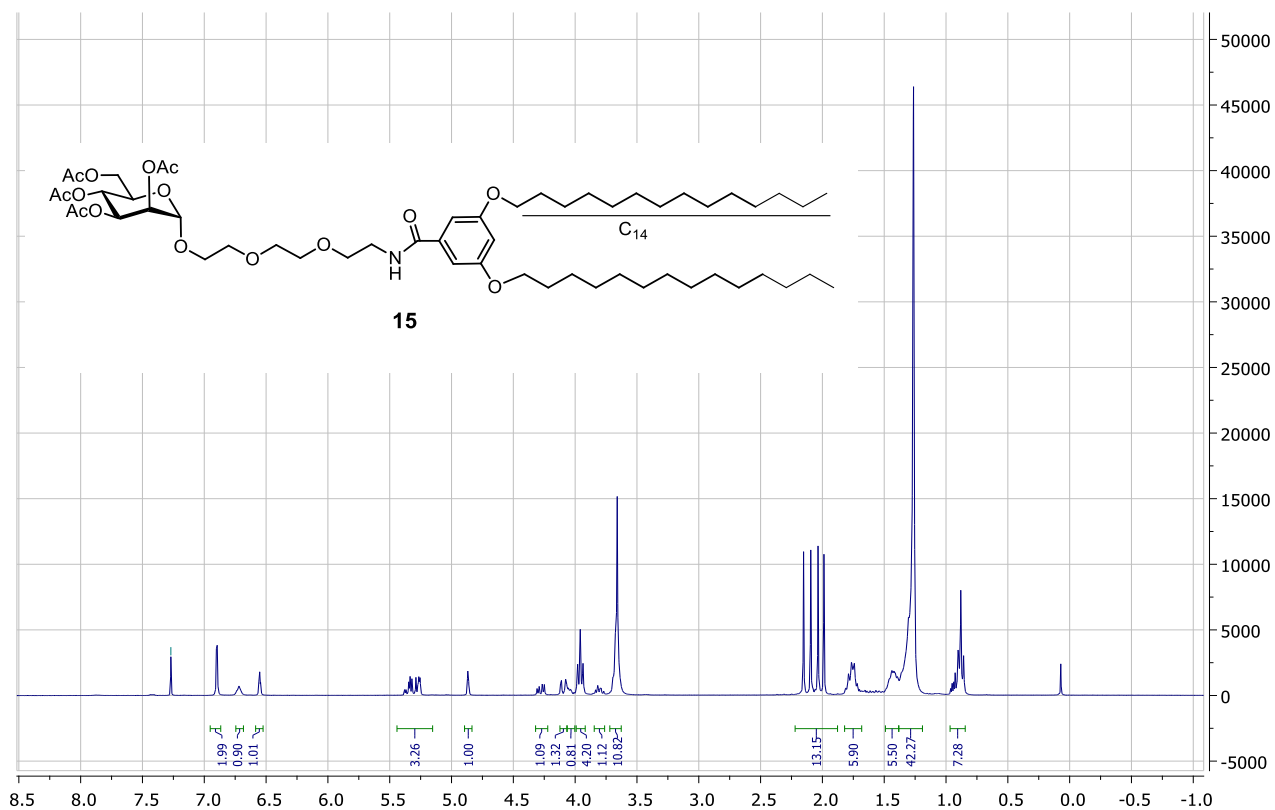


Figure 23. $^1\text{H-NMR}$ (600 MHz, CDCl_3) of compound **15**

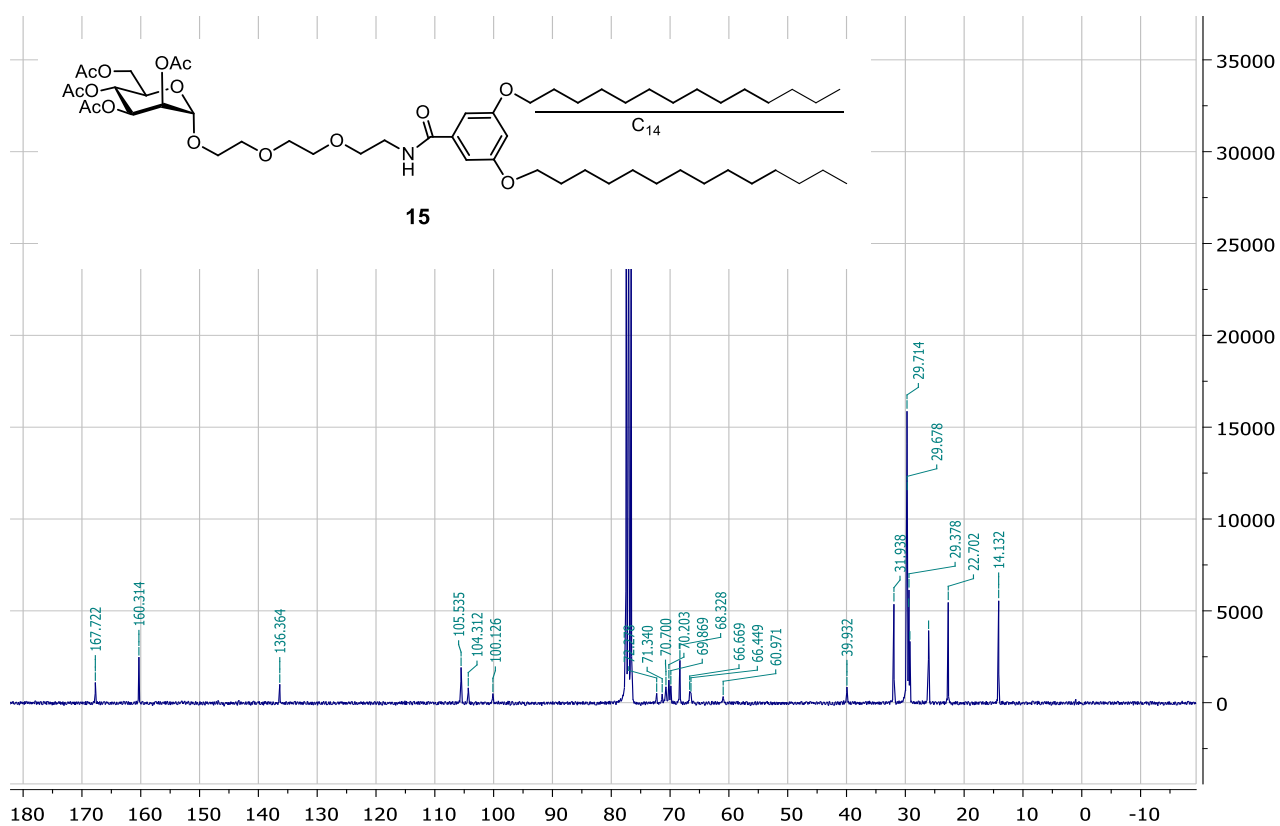


Figure 24. $^{13}\text{C-NMR}$ (75 MHz, CDCl_3) of compound **15**

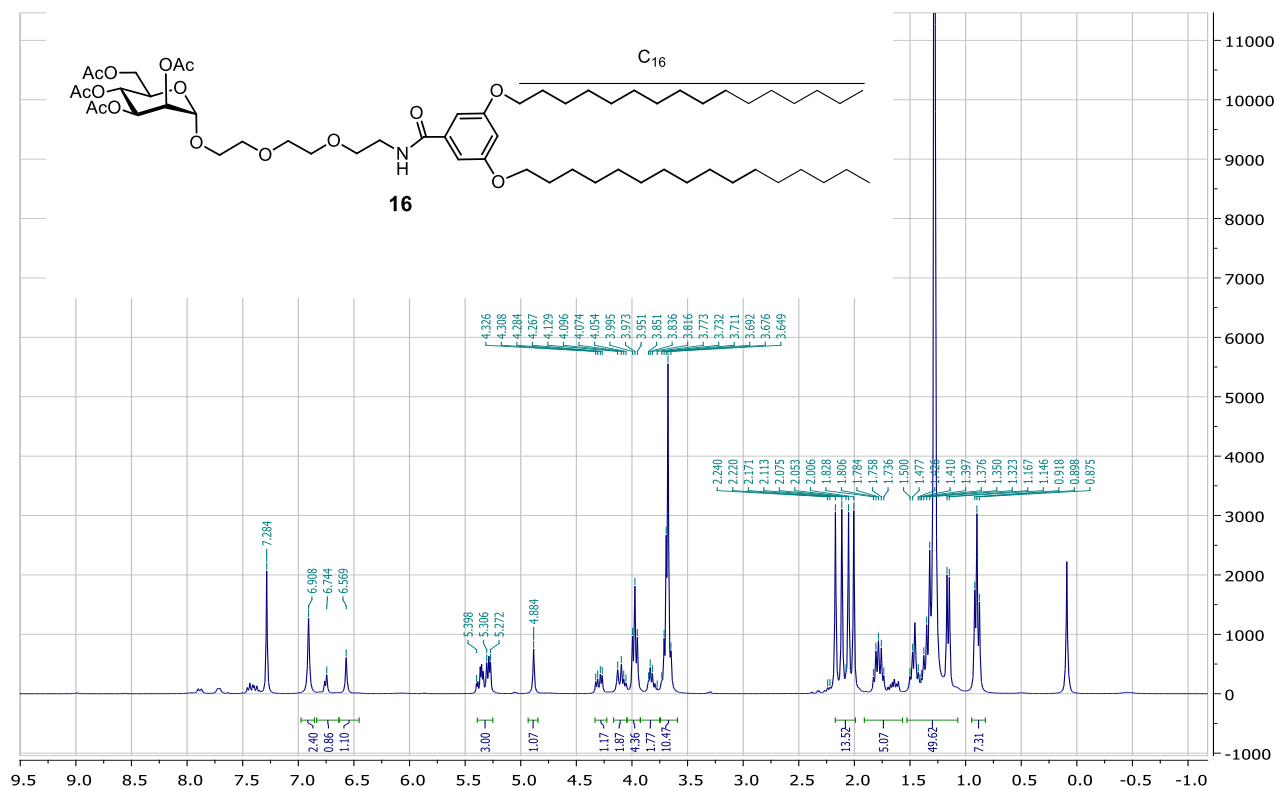


Figure 25. ¹H NMR (600 MHz, CDCl₃) of compound 16

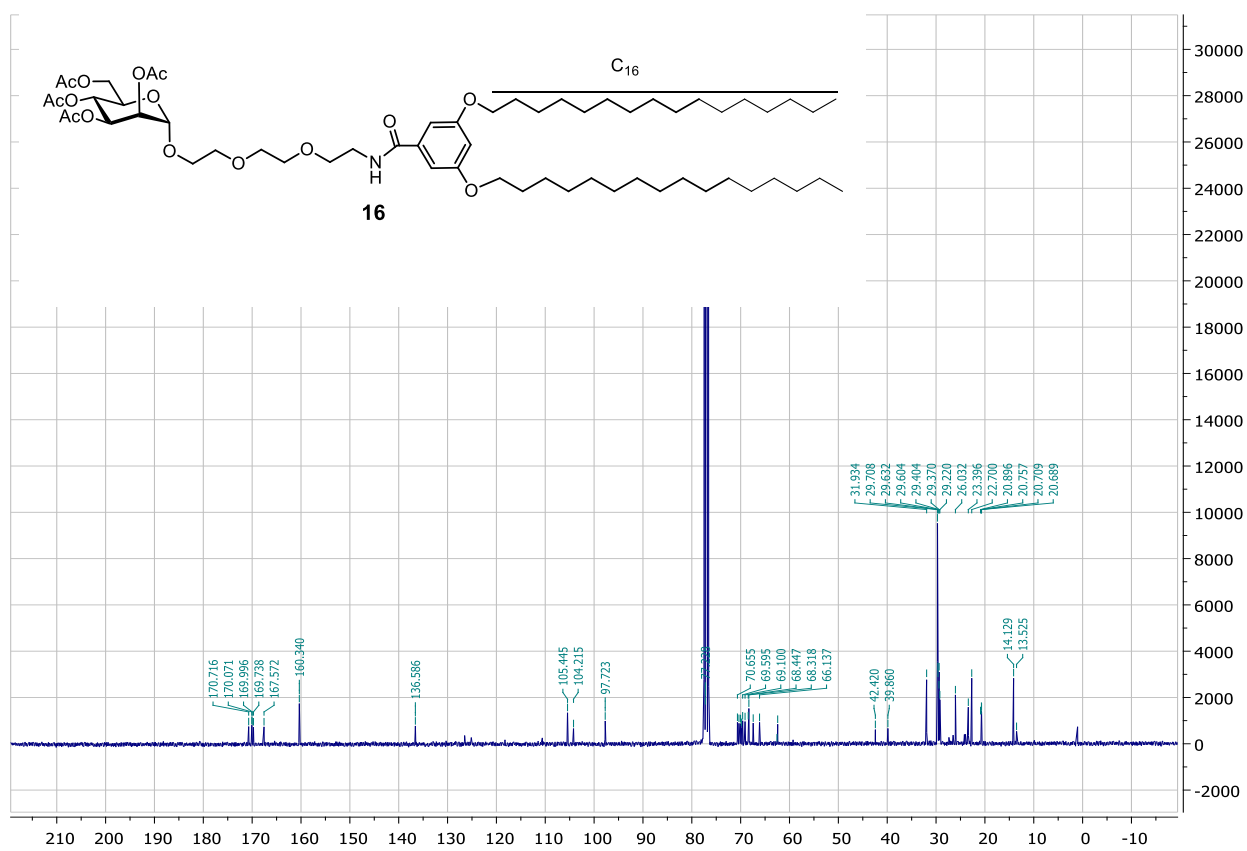
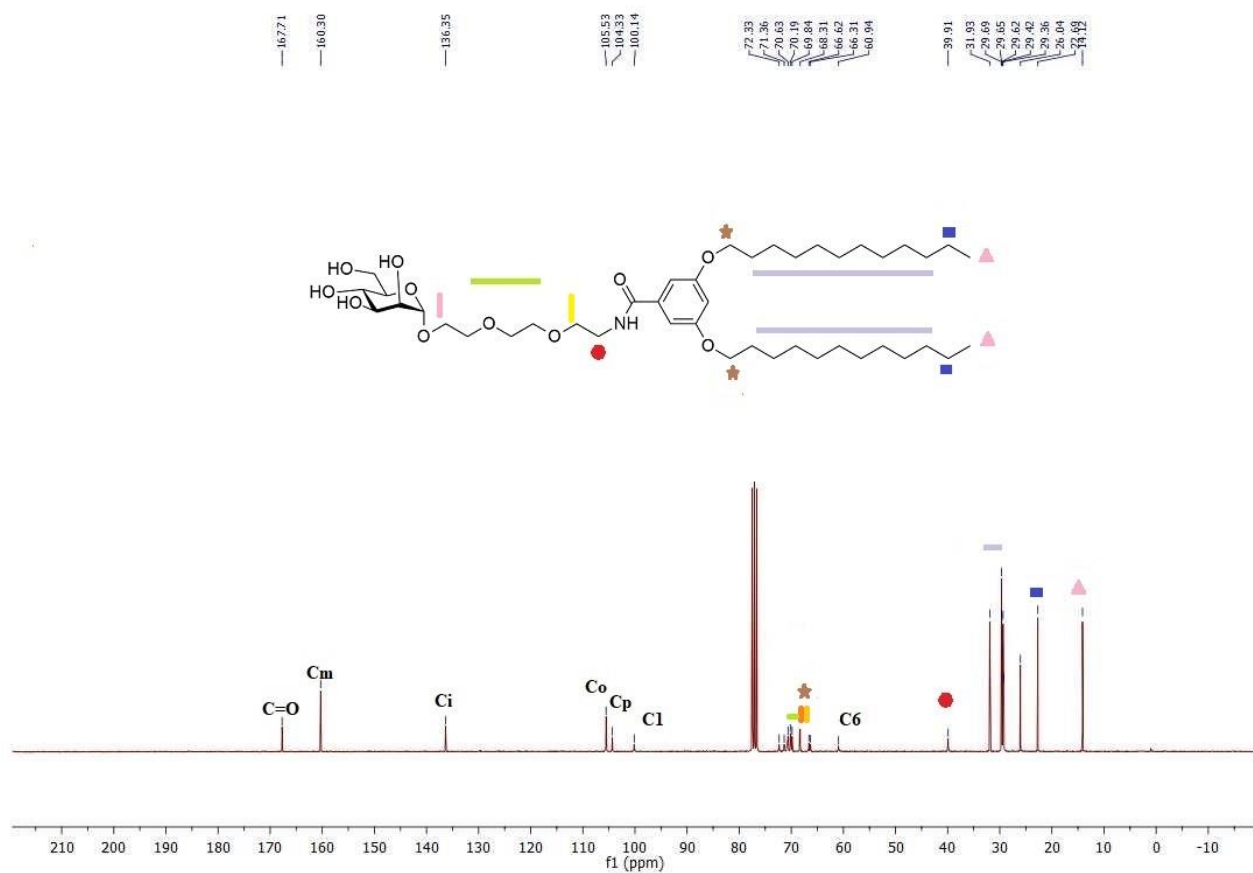
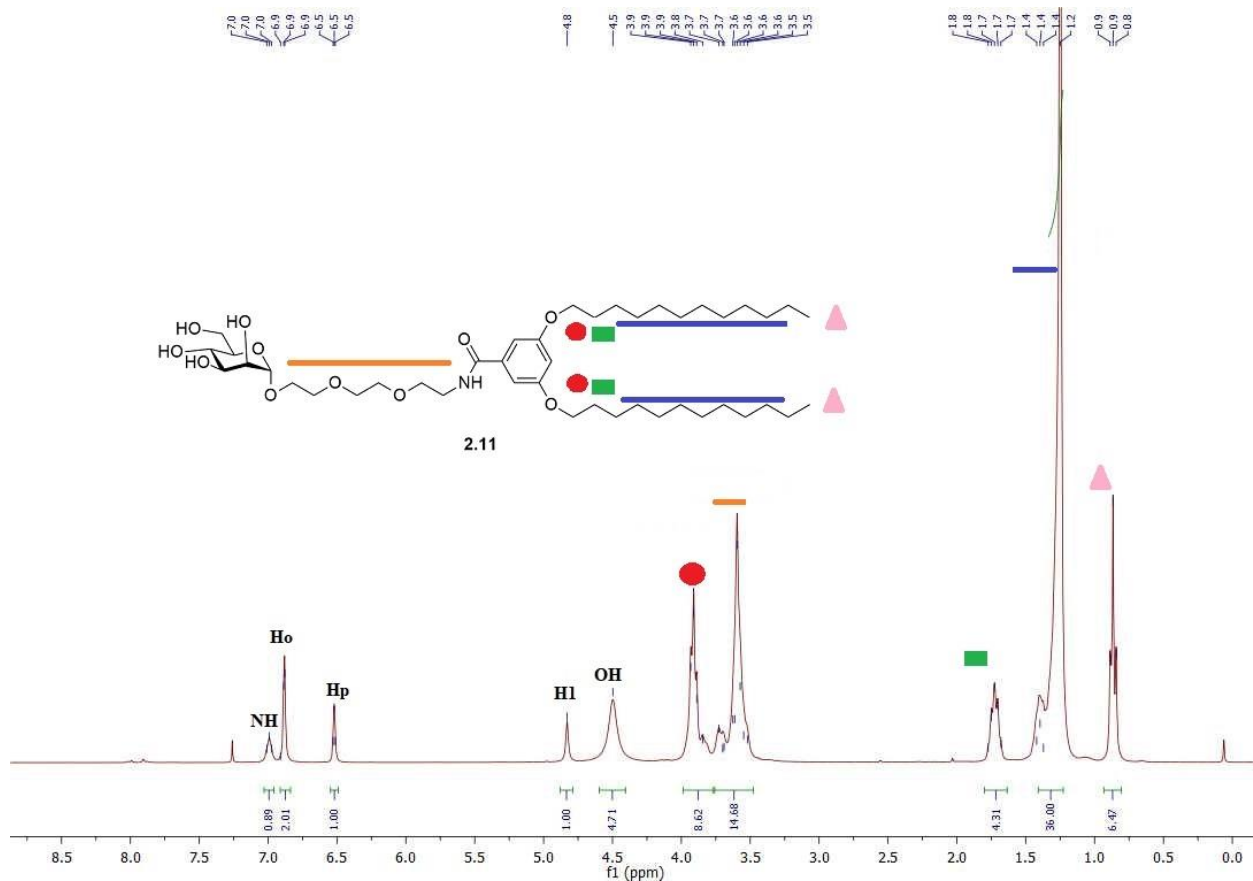


Figure 26. ¹³C-NMR (75 MHz, CDCl₃) of compound 16



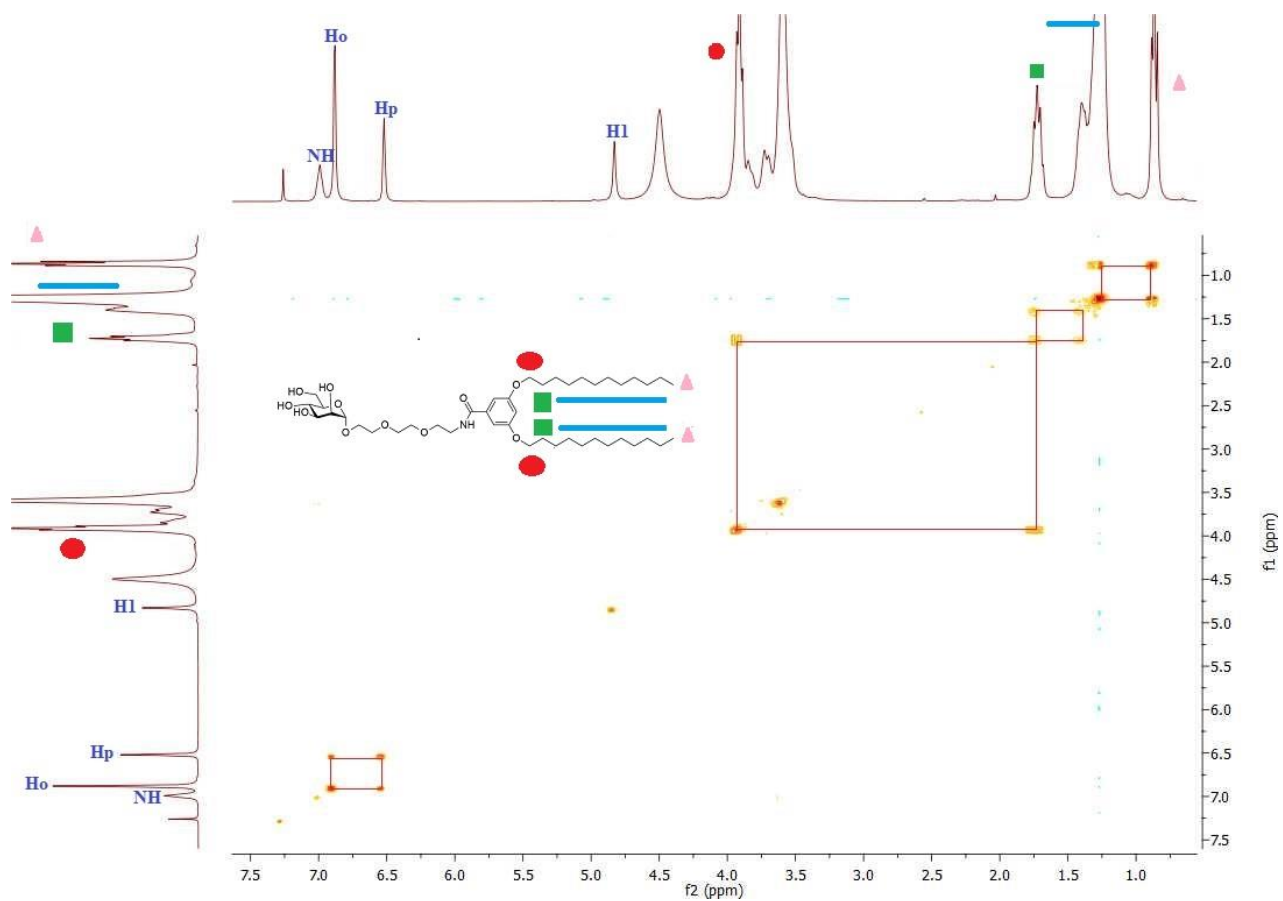


Figure 29. 2D NMR-COSY ^1H - ^1H of compound 17

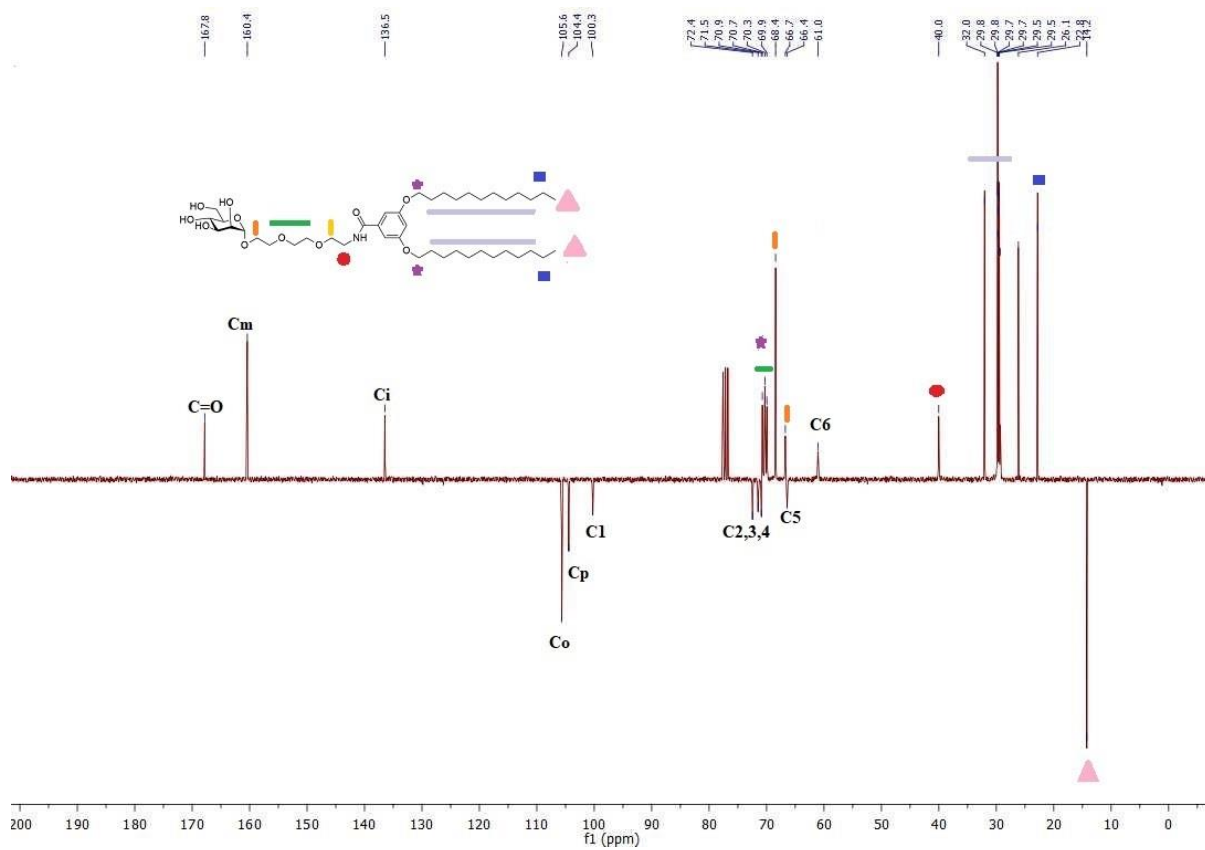
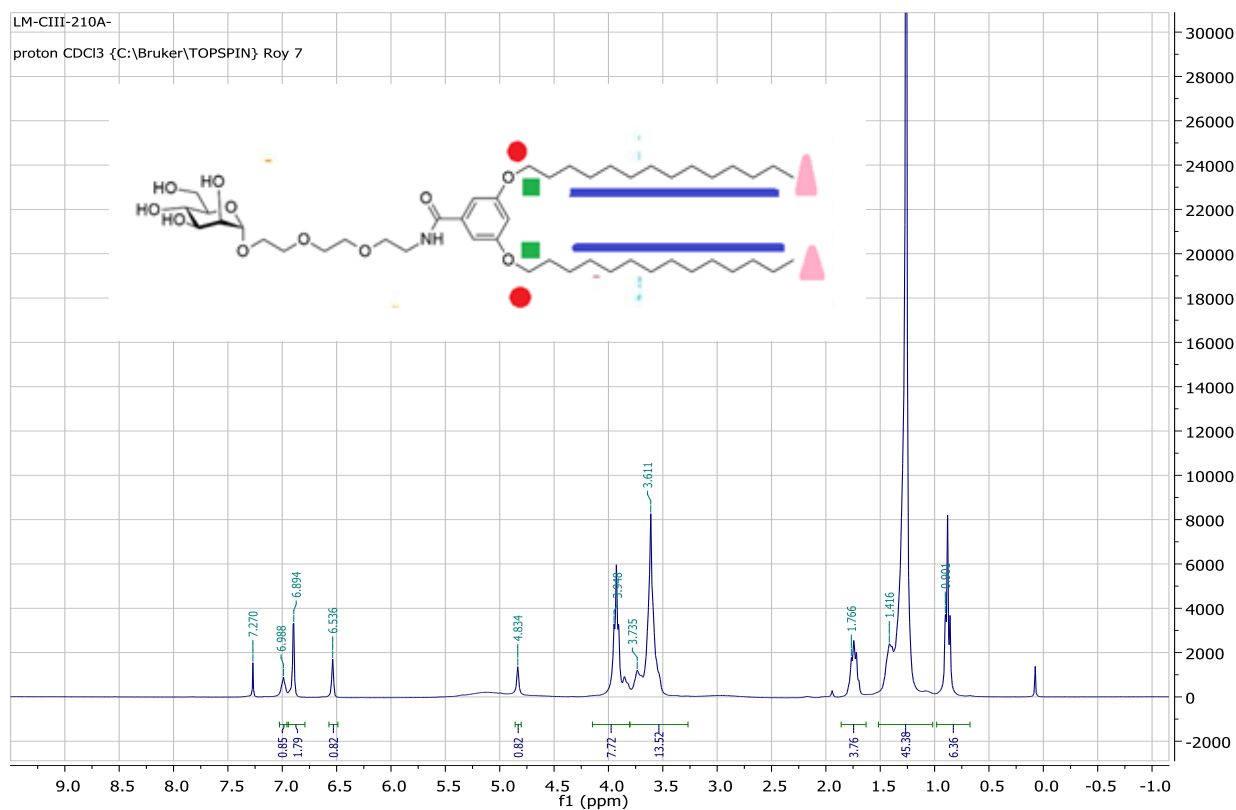
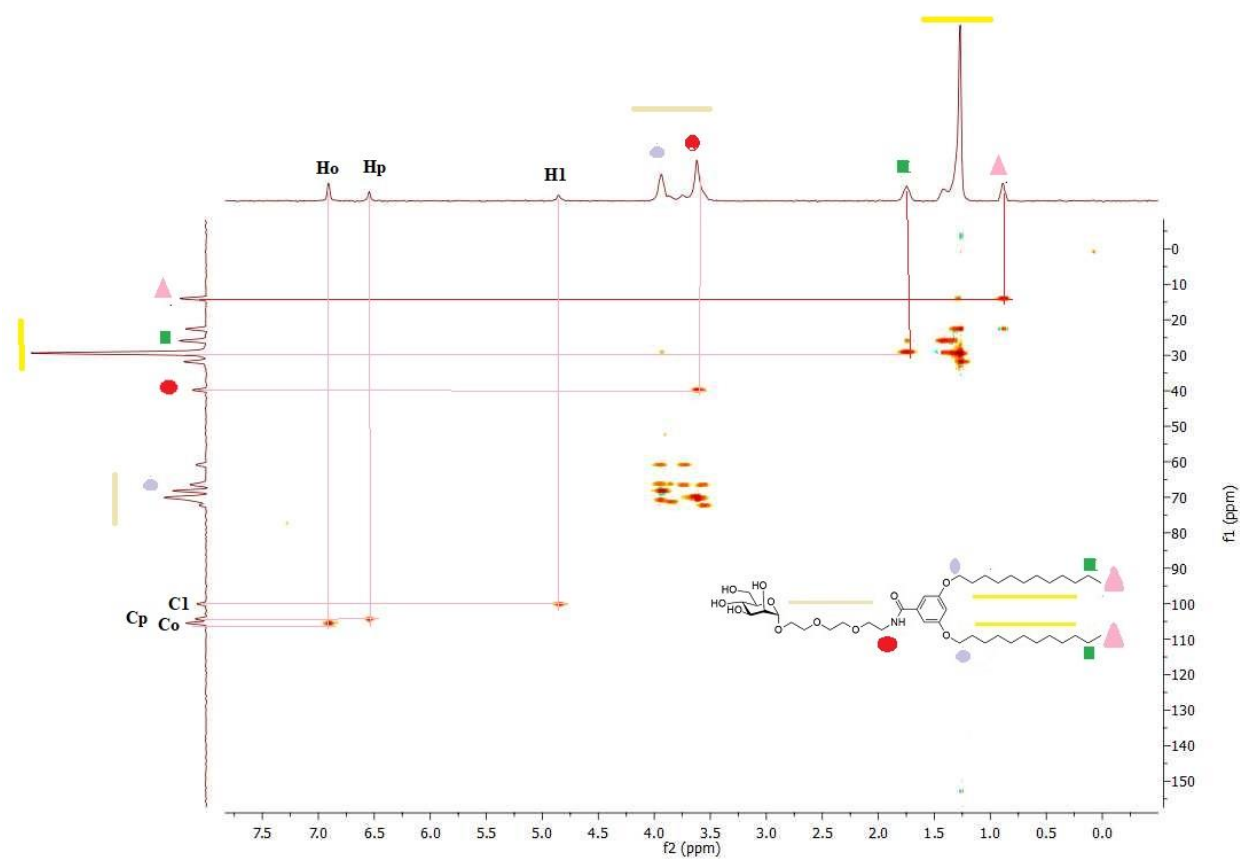


Figure 30. DEPT-135 NMR of compound 17



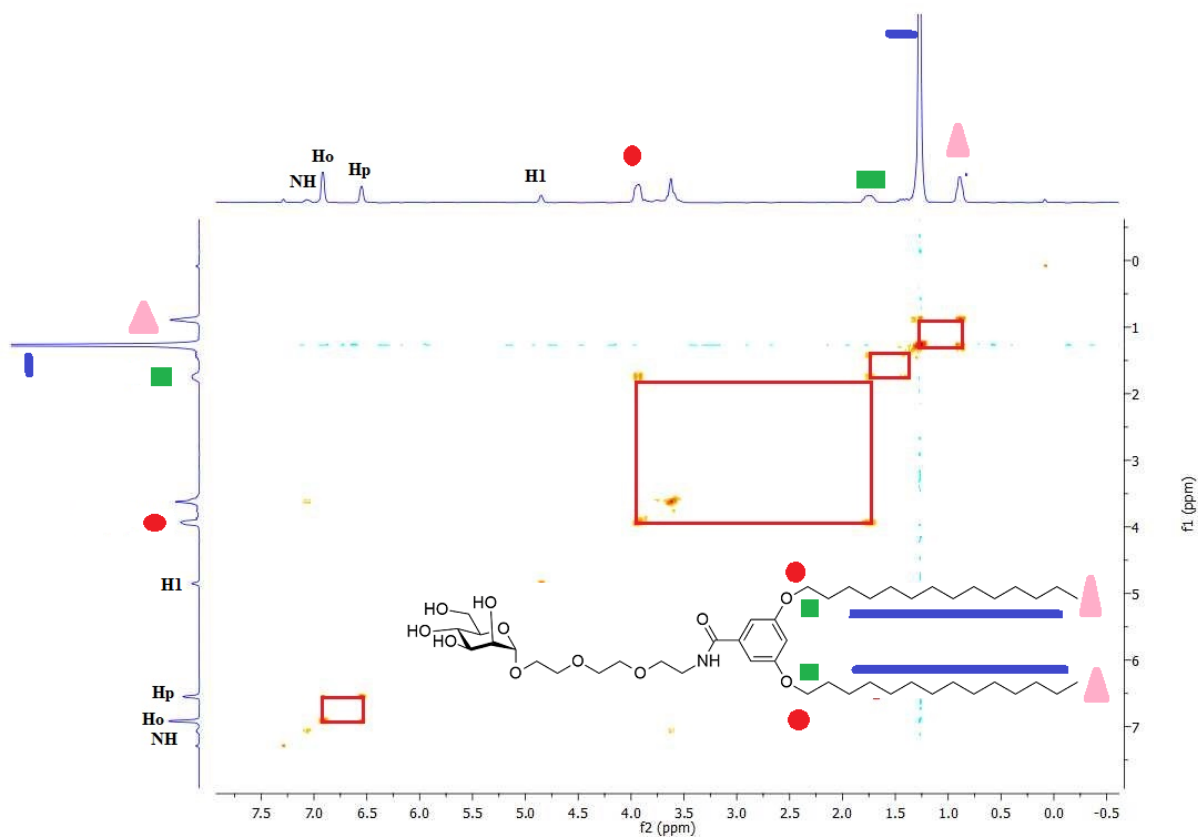


Figure 32. 2D NMR-COSY ^1H - ^1H of compound 18

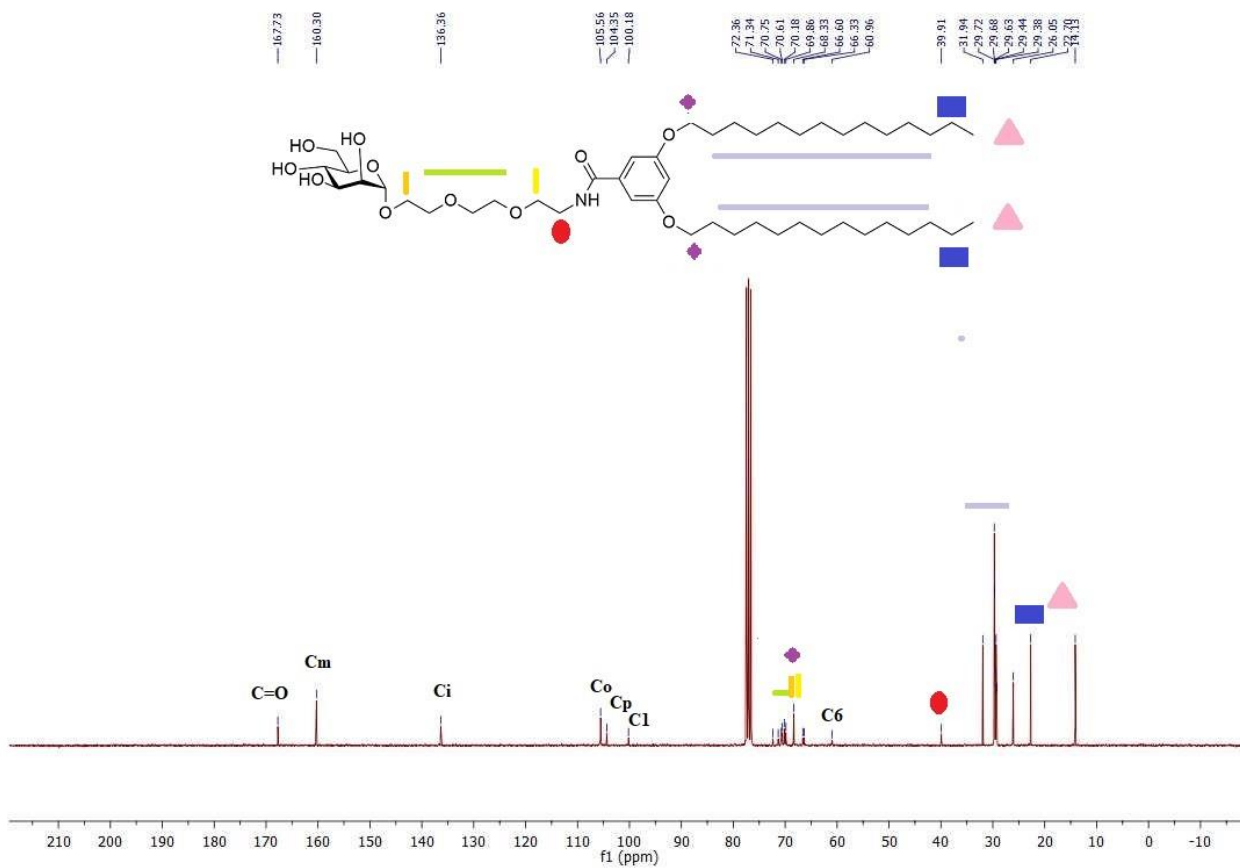


Figure 33. ^{13}C NMR (300 MHz, CDCl_3) of compound 18

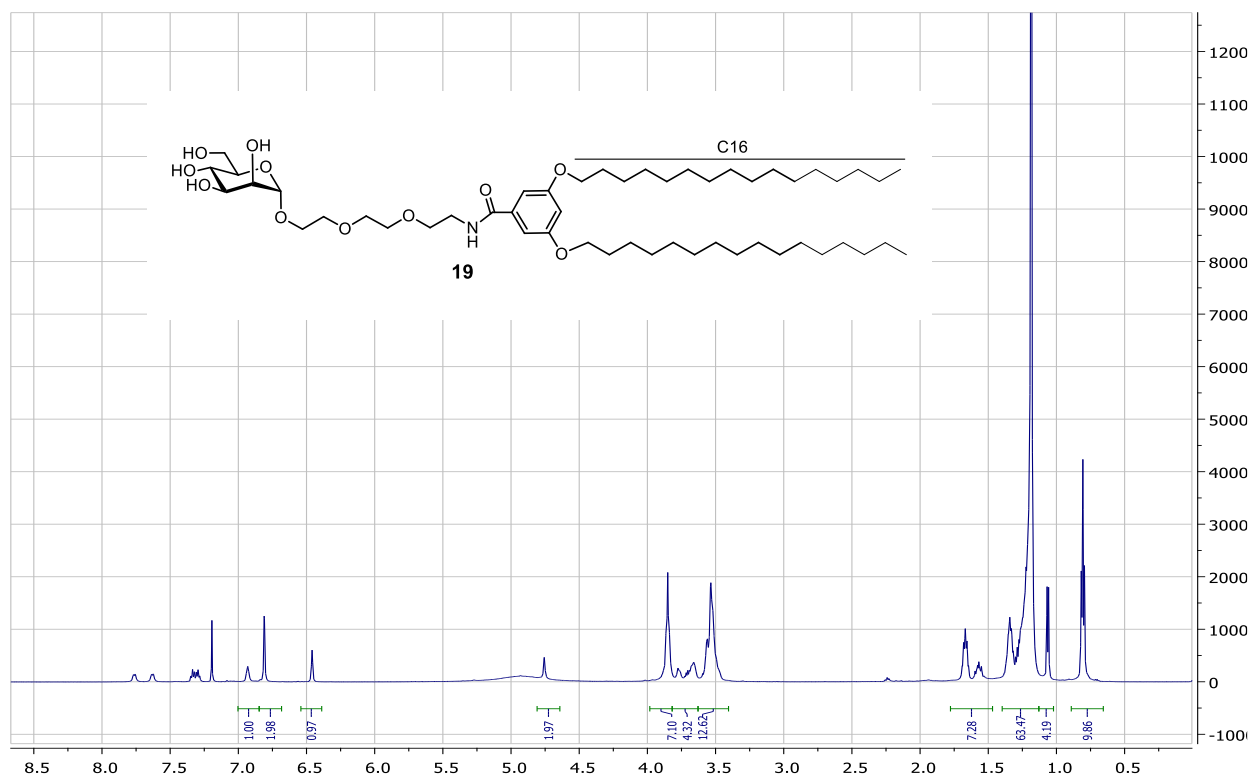


Figure 34. ^1H NMR (600 MHz, CDCl_3) of compound **19**

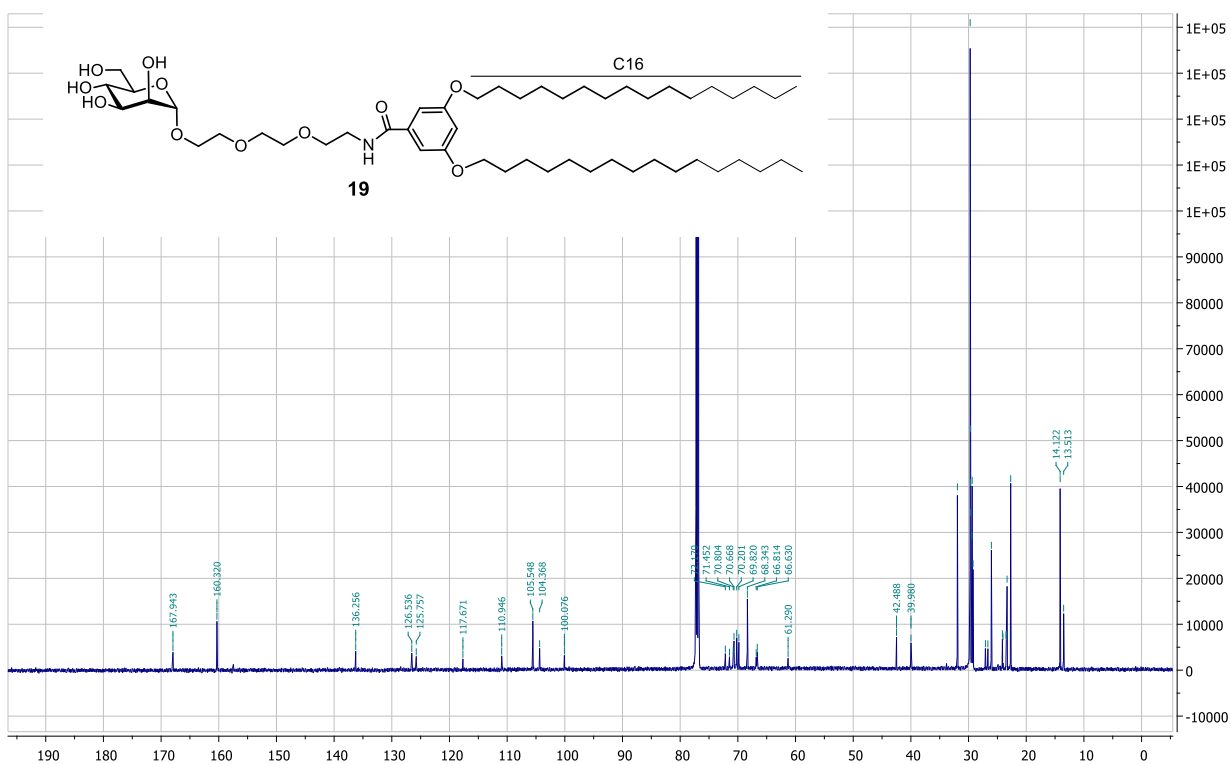


Figure 35. ^{13}C NMR (75 MHz, CDCl_3) of compound **19**

Critical Micelle Concentration (CMC):

CMCs were determined using a Malvern Zetasizer Ultra (MAL1301351) (Malvern Instruments Limited, U.K.) equipped with a 4 mW He–Ne laser operating at a wavelength of 633nm. Scattered light was detected at an angle of 173°, an optical arrangement known as non-invasive back scatter (NIBS) optic arrangement that maximizes the detection of scattered light while maintaining signal quality. Measurements were carried out in a (DTS0012) polystyrene latex cell at 25 °C. A series of solutions ranging from 5×10^{-4} to 0.044×10^{-5} mol/L was prepared from an aqueous stock solution prepared at initial concentration of 1 mg/mL of compound **17-19** in ethanol followed by 2-fold dilution in distilled water. Data processing was carried out with a computer attached to the instrument. The measurements were repeated three times in order to check their reproducibility.¹

The CMC values for mannolipids **17-19** were 1.76×10^{-6} , 3.87×10^{-6} , and 3.86×10^{-6} mole/L, respectively.

References

1. Önder Topel, Burçin Acar Çakır, Leyla Budama, Numan Hoda. Determination of critical micelle concentration of polybutadiene-block-poly(ethyleneoxide) diblock copolymer by fluorescence spectroscopy and dynamic light scattering. *J. Molec. Liq.*, **2013**, 177, 40–43.

Table 1. Scattered intensity (kcps) as a function of mannolipid **17** (C12) concentration (mol/L).

Entry	Concentration (mol/L)	Concentration (mol/L) $\times 10^{-5}$	Intensity per kcps
1.	0.044×10^{-5}	0.044	4.83
2.	0.088×10^{-5}	0.088	4.84
3.	0.098×10^{-5}	0.098	4.84
4.	0.110×10^{-5}	0.011	4.83
5.	0.126×10^{-5}	0.126	4.84
6.	0.147×10^{-5}	0.147	4.84
7.	0.176×10^{-5}	0.176	4.91
8.	0.220×10^{-5}	0.220	5.11
9.	0.441×10^{-5}	0.441	8.43
10.	2.23×10^{-5}	2.23	35.7
11.	0.455×10^{-4}	4.55	73.1
12.	0.945×10^{-4}	9.45	88.8
13.	1.47×10^{-4}	14.7	119.3
14.	2.04×10^{-4}	20.4	131.1
15.	2.65×10^{-4}	26.5	143.6
16.	3.32×10^{-4}	33.2	159.0
17.	4.06×10^{-4}	40.6	171.1
18.	4.86×10^{-4}	48.6	207.3
19.	5.74×10^{-4}	57.4	219.0

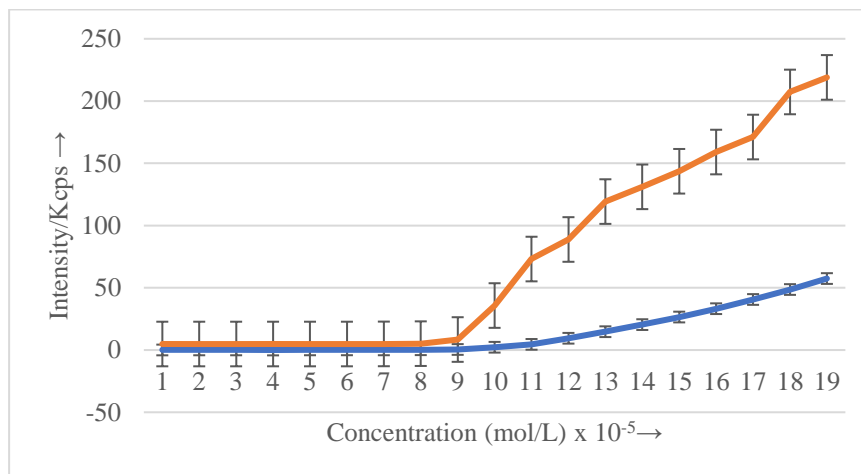


Table 2. Scattered intensity (kcps) as a function of mannolipid **18** (C14) concentration (mol/L).

Entry	Concentration (mol/L)	Concentration (mol/L) x 10 ⁻⁵	Intensity per kcps
1.	0.0387 x 10 ⁻⁵	0.0387	5.33
2.	0.0774 x 10 ⁻⁵	0.0774	5.34
3.	0.0860 x 10 ⁻⁵	0.0860	5.35
4.	0.0968 x 10 ⁻⁵	0.0968	5.33
5.	0.11 0 x 10 ⁻⁵	0.110	5.34
6.	0.129 x 10 ⁻⁵	0.129	5.34
7.	0.154 x 10 ⁻⁵	0.154	5.33
8.	0.193 x 10 ⁻⁵	0.193	5.35
9.	0.387 x 10⁻⁵	0.387	7.37
10.	1.95 x 10 ⁻⁵	1.95	35.6
11.	0.400 x 10 ⁻⁴	4.00	50.6
12.	0.829 x 10 ⁻⁴	8.29	69.7
13.	1.29 x 10 ⁻⁴	12.9	115.8
14.	1.79 x 10 ⁻⁴	17.9	140.7
15.	2.22 x 10 ⁻⁴	22.2	164.7
16.	2.92 x 10 ⁻⁴	29.2	206.4
17.	3.56 x 10 ⁻⁴	35.6	285.1
18.	4.24 x 10 ⁻⁴	42.4	300.5
19.	5.04 x 10 ⁻⁴	50.4	317.3

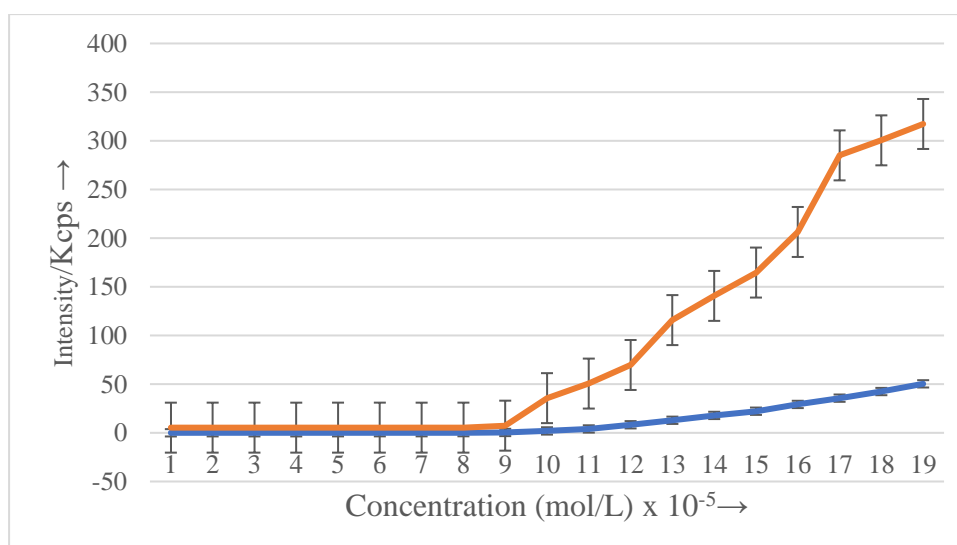


Table 3. Scattered intensity (kcps) as a function of mannolipid **19** (C16) concentration (mol/L).

Entry	Concentration (mol/L)	Concentration (mol/L) x 10 ⁻⁵	Intensity per kcps
1.	0.0386 x 10 ⁻⁵	0.0386	5.54
2.	0.0772 x 10 ⁻⁵	0.0772	5.55
3.	0.0857 x 10 ⁻⁵	0.0857	5.55
4.	0.0965 x 10 ⁻⁵	0.0965	5.55
5.	0.1102 x 10 ⁻⁵	0.1102	5.55
6.	0.128 x 10 ⁻⁵	0.128	5.56
7.	0.154 x 10 ⁻⁵	0.154	5.57
8.	0.193 x 10 ⁻⁵	0.193	5.57
9.	0.386 x 10⁻⁵	0.386	7.93
10.	1.96 x 10 ⁻⁵	1.96	34.6
11.	0.400 x 10 ⁻⁴	4.00	51.6
12.	0.826 x 10 ⁻⁴	8.26	70.7
13.	1.29 x 10 ⁻⁴	12.9	117.9
14.	1.78 x 10 ⁻⁴	17.8	151.0
15.	2.32 x 10 ⁻⁴	23.2	168.6
16.	2.91 x 10 ⁻⁴	29.1	209.3
17.	3.55 x 10 ⁻⁴	35.5	265.2
18.	4.25 x 10 ⁻⁴	42.5	298.4
19.	5.02 x 10 ⁻⁴	50.2	328.4

